Roy, Soumya; Nellattukuzhi Sreenivasan, Harisankar; Sarmah, Ajit K.; Baniasadi, Hossein; Bordoloi, Sanandam

Recent advances for CO2 mineralization in biochar-amended cementitious composites

Published in:
Resources, Conservation and Recycling

DOI:
10.1016/j.resconrec.2025.108141

Published: 01/04/2025

Document Version
Publisher's PDF, also known as Version of record

Please cite the original version:
Roy, S., Nellattukuzhi Sreenivasan, H., Sarmah, A. K., Baniasadi, H., & Bordoloi, S. (2025). Recent advances for CO2 mineralization in biochar-amended cementitious composites. *Resources, Conservation and Recycling*, *215*, Article 108141. https://doi.org/10.1016/j.resconrec.2025.108141

Resources, Conservation & Recycling 215 (2025) 108141

Contents lists available at ScienceDirect

Resources, Conservation & Recycling

journal homepage: www.sciencedirect.com/journal/resources-conservation-and-recycling

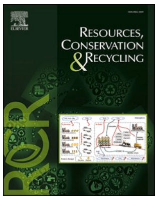

Review

Recent advances for CO_2 mineralization in biochar-amended cementitious composites

Soumya Roy [a], Harisankar Sreenivasan [a,b], Ajit K Sarmah [c], Hossein Baniasadi [d], Sanandam Bordoloi [a,*]

[a] *Department of Civil Engineering, Aalto University, Finland*
[b] *Advanced Infrastructure Materials Laboratory, Dept. of Civil and Environmental Engineering, Imperial College London, South Kensington, London SW7 2AZ, UK*
[c] *Faculty of Engineering, Department of Civil and Environmental Engineering, University of Auckland, New Zealand*
[d] *Department of Chemical Engineering, Aalto University, Finland*

ARTICLE INFO

Keywords:
CO_2 mineralization
Biochar
Accelerated co2 curing
Low carbon cementitious composite

ABSTRACT

Biochar, a carbonaceous material derived from organic waste, has recently been explored to mitigate the negative effects of accelerated carbon-di-oxide (CO_2) curing (ACC) on concrete properties. This review categorizes the literature on biochar-amended cementitious composites and examines the key mechanisms governing CO_2 mineralization. The influence of CO_2 phases (gaseous and liquid) on mineralization during curing is discussed, focusing on how altering CO_2 pressure and temperature can enhance the process. We explore the role of biochar's surface functional groups, aromaticity, porosity, and honeycomb structures in both carbonation and hydration. Additionally, the properties of the cementitious matrix—such as saturation degree, porosity, and ideal amorphous phases—are shown to improve carbonation. Despite these advancements, several gaps remain before biochar-amended composites can be adopted as conventional construction materials. These include the development of homogeneous biochar, standardization of ACC conditions, and the assessment of end-of-life leaching. The review highlights that strength gains of up to 71 % and CO_2 uptake levels of up to 13 % are achievable in biochar-amended cementitious composites. Furthermore, the knowledge from other hydrocarbon-based materials in the petroleum industry is discussed to better understand the complex interactions of gas-air-solid flow during ACC.

1. Introduction

In September 2023, the United Nations Environment Program (UNEP) reported that the construction industry is by far the biggest emitter (37 %) of all greenhouse gas emissions. In particular, the preparation of Ordinary Portland cement (OPC), a globally used binder, creates 0.8 to 1 ton of carbon dioxide (CO_2) per ton of cement (Zhang et al., 2023). Considerable work has been done to promote sustainable construction practices (S. Baradaran et al. 2024, Nilimaa 2023, Khan M. and McNally C. 2023, Abdullah M. Zeyad 2023, Sathiparan et al. 2023, S. Baradaran et al. 2024). The European Union has set a target to achieve "net zero" CO_2 emissions by 2050 (L. Chen et al. 2022). Cutting existing emission levels will have a significant role in reaching this goal. Additionally, new technologies and approaches are needed to systematically capture CO_2 from the environment and store it in a stable form.

Carbon capture, utilisation, and storage (CCUS) is an umbrella term used to define technologies that sequester atmospheric CO_2 in a stable form and ultimately reduce greenhouse gas emissions (Zhang et al. 2022). Fig. 1 shows the three primary phases of CCUS technology. During the capture phase, CO_2 is separated from mixed industrial

---

Abbreviations: ACC, Accelerated carbonation curing; $CaCO_3$, Calcium carbonate; CCUS, Carbon capture utilization and storage; CO_2, Carbon dioxide; C_2S, Dicalcium silicate; C_3S, Tricalcium silicate; C_3A, Tricalcium aluminate; C_4AF, Tetracalcium aluminoferrite; OPC, Ordinary Portland cement; SCMs, Supplementary cementitious materials; AFm, Calcium aluminoferrite hydrate; AFt, Calcium aluminate trihydrate; CH, Calcium hydroxide; C-S-H, Calcium silicate hydrate; TGA, Thermogravimetric analysis; DTG, Differential thermogravimetric analysis; CEC, Cation exchange capacity; $scCO_2$, Supercritical CO_2; RH, Relative humidity; UN, United Nations.

[*] Corresponding author.
E-mail addresses: soumya.roy@aalto.fi (S. Roy), a.sarmah@auckland.ac.nz (A.K. Sarmah), hossein.baniasadi@aalto.fi (H. Baniasadi), sanandam.bordoloi@aalto.fi (S. Bordoloi).

https://doi.org/10.1016/j.resconrec.2025.108141
Received 3 October 2024; Received in revised form 27 December 2024; Accepted 19 January 2025

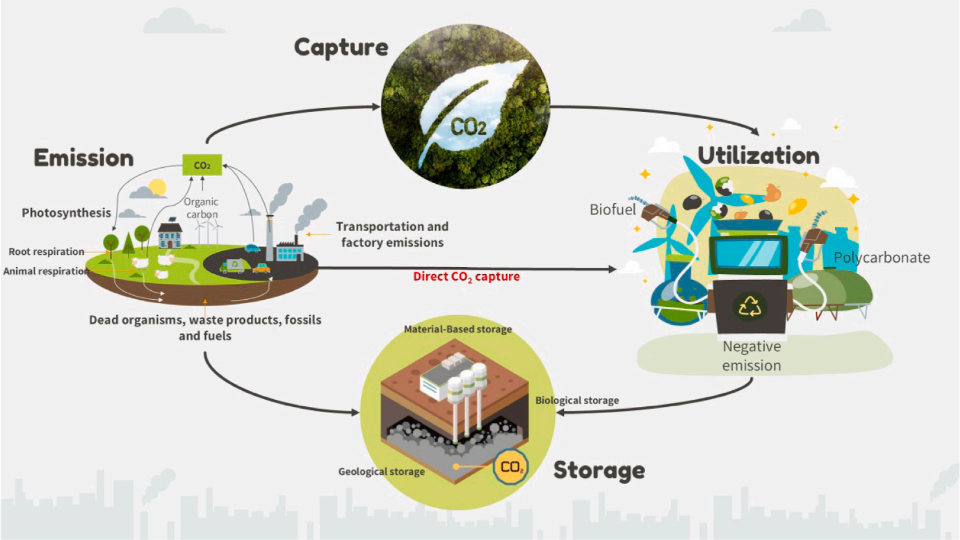

Fig. 1. Carbon capture utilization and storage strategies for sequestering CO_2.

emissions through processes like pre-combustion, post-combustion, or oxy-fuel combustion, each offering unique benefits and drawbacks (Kheirinik et al. 2021). The captured CO_2 can be subsequently valorised in a range of applications, including (1) supercritical CO_2 as a reactive solvent, (2) mineralization of CO_2 in supplementary cementitious materials (SCMs) as inorganic carbonates, (3) catalytic reduction of CO_2 into organic fuel for transport, (4) transformation of CO_2 to value-added chemicals, and (5) biological CO_2 utilization; converting a waste product into an important resource (Pan et al. 2018). Lastly, any CO_2 that is not needed is stored in geological formations like deep saline aquifers, depleted oil and gas fields, or exhausted coal seams. However, this process of underground carbon storage, also known as geological carbon sequestration, is costly given the advanced technology, monitoring, infrastructure development, and ensuring long-term containment to prevent leakage (Xie and Economides 2009).

Biochar is a carbon-rich, eco-friendly adsorbent material made from the pyrolysis of biomass, which can be used to improve CO_2 sequestration in cementitious materials (Akinyemi and Adesina 2020). Because of its high surface area and porous structure, biochar is a very useful medium for absorbing CO_2, either directly through physical adsorption or indirectly through chemical processes that result in the formation of stable carbonates (Zhang et al. 2022). Accelerated carbonation curing (ACC), an innovative method for curing pre-cast concrete, can significantly reduce CO_2 emissions in the cement industry. This process sequesters CO_2, converting it into stable products within the concrete, transforming the construction materials into a sink rather than emitters (Sharma and Goyal 2018; Wang et al. 2021). However, there are roadblocks of directly sequestering CO_2 in concrete blocks as it does not necessarily benefit the mechanical properties of the cement-based composites with the carbonated materials. For instance, for a specific material, a threshold may exist, after which there might be pore blockage, resulting in partial hydration of concrete, which can be deleterious for its mechanical properties (Li and Wu 2022). To improve the overall CO_2 diffusion in concrete matrix, new materials are being envisioned to enhance CO_2 diffusion in cementitious composites, including options like carbon nanotubes, cellulose, and biochar (Escobar et al. 2013; Reyes et al.2023; Song et al. 2023). Much emphasis has been placed in recent years on utilising biochar as a carbon-negative material and adding it to cementitious materials to enhance concrete's mechanical qualities by improving cement hydration, enabling CO_2 mineralization, and lowering the carbon impact on the construction industry (Mishra et al. 2023). Studies have demonstrated the potential of biochar-amended cementitious materials to absorb and retain CO_2 during the carbonation and hydration processes. Further, biochar can

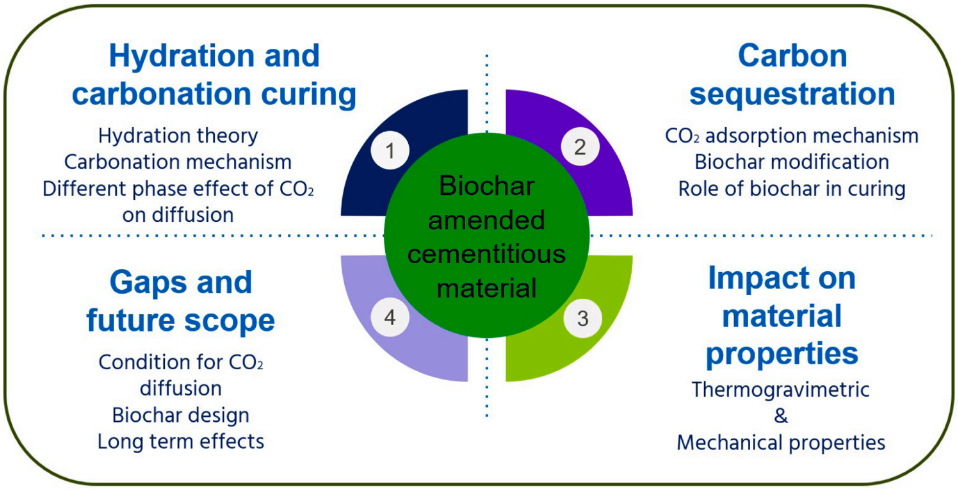

Fig. 2. Flow chart of biochar amended cementitious composites.

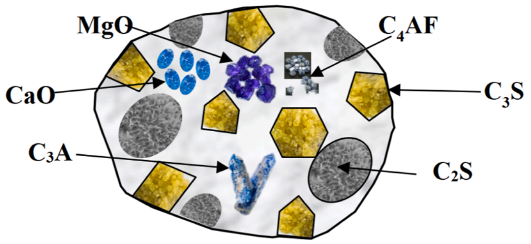

Typical cement clinker with non-hydrated constituents

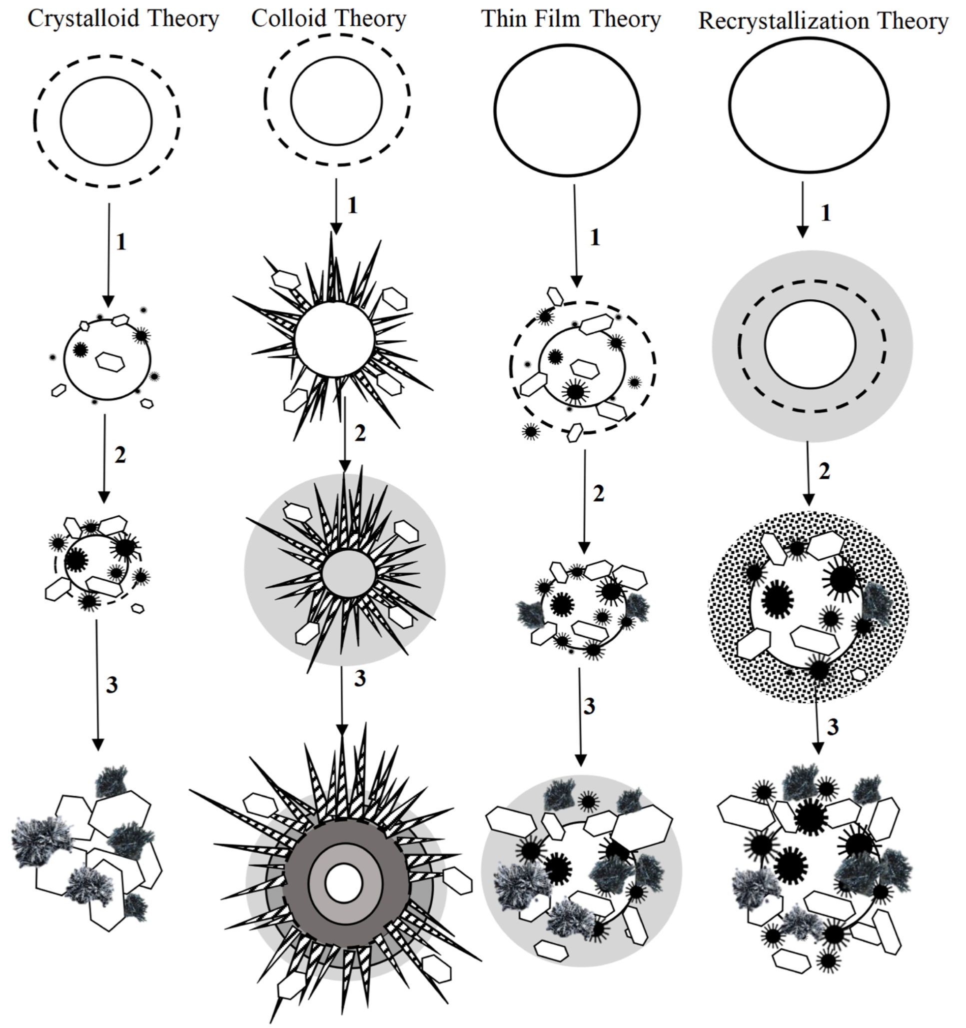

Fig. 3. Some idealistic cement hydration theory occurring in cementitious composites.

also be modified to increase its reactivity and CO_2 sequestration capacity with specific elements, such as doping it with calcium or magnesium (Nan et al. 2020). However, challenges remain, such as optimizing the conditions for CO_2 diffusion and creating standardized pyrolysis conditions for preparing suitable biochar for widespread use in the construction industry.

There have been four review articles on biochar usage in concrete in the recent past (Tan et al., 2022; Senadheera et al., 2023; Singhal 2023; Barbhuiya et al., 2024) that focussed more on biochar's use as a filler or as an agent that changes hydration products. In the current study, we discuss the potential mechanisms by which CO_2 mineralization can be accelerated in cementitious construction materials with a CCUS strategy. Unique concepts and mechanisms from petroleum industry-based CO_2 mineralization strategies have also been put forward to gauge a scientific understanding of biochar as a catalyst for CO_2 capture in cementitious materials.

2. Methodology

The literature on CO_2 mineralization in biochar-amended cementitious composites is broad and interdisciplinary. We focus primarily on the publications having keywords "biochar amended cement", "biochar amended concrete", "accelerated CO_2 curing", "hydration", "CO_2 diffusion", "Carbonate formation", "low carbon concrete", "supplementary cementitious materials", "carbon amended concrete", "biochar" and "CO_2 mineralization". More than >150 publications on the

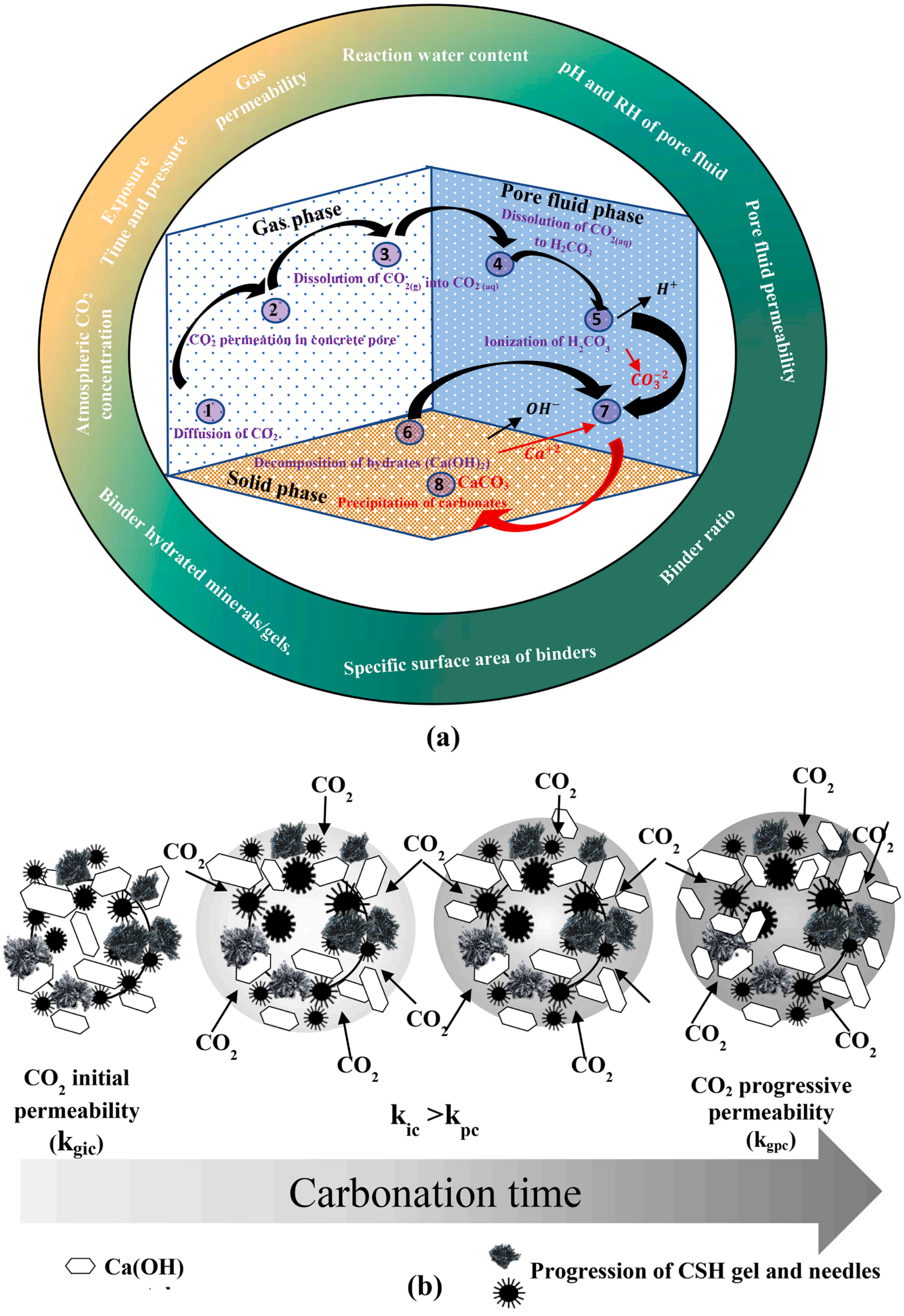

Fig. 4. (a) Schematic illustration of the carbonation pathway through three phases and associated factors affecting the quantity and rate of CO_2 mineralization. (b) CO_2 permeability changes over time during the carbonation process.

keywords given above have been reviewed in this paper, considering work not only in concrete but also in CO_2 sequestration in hydrocarbon materials. The selection was based on their relevance to our study objectives, publication in peer-reviewed sources, and the novelty of their contributions. We limit the review to peer-reviewed papers in science citation-indexed scientific journals, technical conference proceedings, and peer-reviewed books on relevant topics and exclude any grey literature. The scientific databases used for relevant searches in this reviewed work include primarily “Science Direct”, “Science Citation Index Expanded”, “Google scholar”, “Mendeley” and “Scopus”.

The research methodology adopted in this review is illustrated schematically in Fig. 2. A thorough assessment is done on how biochar can act as a catalyst for CO_2 sequestration in cementitious materials, focusing not only on its role as an aggregate for enhancing mechanical and thermal properties but also on its potential to improve CO_2 sequestration in construction materials. Specifically, we explore the mechanisms by which biochar contributes to the carbonation and hydration processes in cementitious composites, highlighting its unique structural properties such as high porosity, surface area, and functional groups. The research conducted over the past six years on biochar-amended cementitious materials for CO_2 sequestration is considered, aiming to uncover the causes and factors that influence CO_2 diffusion mechanisms in these materials (Table A1). Initially, we tried to understand the hydration and carbonation curing processes that influence the overall strength and the factors affecting CO_2 diffusion within the concrete matrix. Following this, we explored how biochar can impact the CO_2 absorption mechanism in cementitious materials and identified potential strategies for enhancing rapid CO_2 sequestration in biochar-amended cementitious materials. Concepts such as the impact of different CO_2 phases on diffusion, internal CO_2 curing, surface modification, external CO_2 curing, and their effects on material properties, including thermogravimetric and mechanical characteristics, are discussed thoroughly. Additionally, we compile a summary of research on biochar-amended cementitious materials and examine how biochar influences strength and overall calcium carbonate ($CaCO_3$) formation. Based on the observed mechanical properties and CO_2 sequestration capabilities of these materials, we identify gaps for future research to explore how these materials can be further improved and highlight areas that need attention before they can be utilised for industrial application.

3. Hydration and carbonation-based curing in cementitious composites

3.1. Cement hydration theory

Cement hydration involves chemical and physical processes associated with the interaction between cement particles and water, leading to the formation of various cementitious phases (Fig. 3). These phases finally undergo hardening and setting to form a solid mass called hydrated cement paste. A critical analysis of cement hydration along with various proposed mechanisms, have been presented in an elaborate manner elsewhere (John and Lothenbach 2023). Chemically, cement particles consist of phases like dicalcium silicate (C_2S), tricalcium silicate (C_3S), tricalcium aluminate (C_3A), and tetra-calcium-aluminoferrite (C_4AF) etc. In the initial stage of hydration, the cement particles dissolve in water, releasing ions into the solution. This leads to the formation of new compounds as the ions interact. As dissolution continues, the concentration of ions in the solution increases until it reaches a state called 'critical oversaturation', where the solution contains more ions than can remain dissolved, causing solid compounds to begin precipitating out. Once this state has been achieved, the nucleation process will ensue, wherein nuclei (of hydrated cementitious phases) start to grow, mainly on the surface of cement particles. This process is influenced by several factors like solubility differences among various phases, modifications of the dissolving surface over time, variations in the concentration of dissolved ions in the solution over time, poisoning effect of chemical species (present in the solution) on the nucleation of hydrated cementitious phases, etc. (John and Lothenbach 2023). Over the past 100 years, numerous mechanisms have been proposed to explain cement hydration processes. Among them, the most prominent and widely accepted are the crystalloid theory, colloid theory, thin film theory, and recrystallization theory, which are demonstrated in Fig. 3 (John and Lothenbach 2023).

3.2. Mechanism of carbonation in cementitious composites

The carbonation of concrete structures can be understood in a simplified manner, focusing on the interplay between CO_2 diffusion, pore fluid interactions, and solid phase reactions (Fig. 4a). It starts with the diffusion of $CO_2(g)$ from the environment into the concrete structure (gas phase). The diffused $CO_2(g)$ permeates through the pores of the concrete and interacts with the pore solution, leading to its aqueous phase formation, followed by its hydration to form carbonic acid in the pore fluid phase. Carbonic acid undergoes reactions that eventually liberate carbonate ions, e.g., hydrogen ions (H^+) and bicarbonate (HCO_3^-), setting the stage for the critical reactions that lead to carbonation. Carbonate ions interact with the cations (derived from the decomposition of their hydrates) and eventually form carbonates. In the solid phase, calcium hydroxide ($Ca(OH)_2$), a key hydration product in cement, decomposes, releasing calcium ions (Ca_2^+). These calcium ions then react with carbonate ions (CO_3^{2-}), precipitating $CaCO_3$. This $CaCO_3$ fills the pores in the concrete, progressively reducing the permeability of CO_2 over time (Fig. 4b). The carbonation process is influenced by several parameters like gas permeability, concrete water content, pH and RH of pore fluid, pore fluid permeability, binder ratio, specific surface area of binders, binder hydrated minerals/gels, atmospheric CO_2 concentration, exposure time and pressure, etc.

All the carbonation reactions can be divided into two categories – "early carbonation reactions" and "late carbonation reactions" (Kua and Tan 2023). "Early carbonation reactions" involve combined hydration and carbonation of C_3S, β-C_2S, γ-C_2S, and MgO. It has been reported that C_3S, β-C_2S, and γ-C_2S exhibit similar reactivity for carbonation (Ashraf and Olek 2016). "Late carbonation reactions" involve the carbonation of hydrated products, calcium hydroxide, calcium silicate hydrate, calcium aluminate hydrate, AFt, and brucite.

The $CaCO_3$ formed during the carbonation reactions is finer, which results in better packing and densification of the cement matrix (Ali et al., 2015). As the cement matrix becomes denser, there is greater water retention, leading to improved cement hydration and, eventually, accelerated hardening and higher early-age strength for the concrete (Ali et al. 2015; Cao et al. 2019). There is an optimum extent of carbonation beyond which carbonation is detrimental to the mechanical and durability properties of concrete due to 1) increased carbonation leading to excessive water consumption and, hence, less water available for essential cement hydration reactions (Gupta et al. 2021; Papadakis 2000), 2) prolonged carbonation resulting in increased decalcification of C—H and C-S-H (Li et al. 2019), and 3) excessive carbonation reducing the pH of pore solution and causing corrosion of steel reinforcement (Angst 2023).

3.3. Factors affecting CO_2 diffusion in a cementitious matrix

3.3.1. Cementitious matrix properties

The diffusion of CO_2 through the concrete pore structure significantly influences carbonation, which begins at the surface and progresses inward, affecting concrete durability. Factors like matrix porosity, tortuosity, water-to-binder ratio, and the interfacial transition zone influence CO_2 diffusion (Cui et al. 2015; Yoon and Chang 2020). Initially, as the CO_2 concentration increases, both diffusion rate and carbonation rate increase, but excessive carbonation leads to pore blockage, reducing diffusivity and carbonation depth due to the formation of $CaCO_3$ and calcium-modified silica gel (Cui et al. 2015). At low CO_2 concentrations (natural carbonation), diffusion dominates, while at high concentrations (accelerated carbonation), Ca ion release from CH or C-S-H becomes critical (García-González et al. 2006). In carbonated concrete, CO_2 diffusivity is initially lower than in uncarbonated concrete due to early pore blockage (Yoon and Chang 2020). Biochar inclusion likely alters CO_2 ingress based on pore CO_2 concentration, highlighting its potential for facilitating CO_2 mineralization in cementitious composites.

Apparent and effective diffusivity is essential to comprehend CO_2 diffusion in concrete. Apparent diffusivity reflects the bulk material's diffusion behaviour under varying environmental conditions, while effective diffusivity focuses on the intrinsic pore network's impact on diffusion (Yoon and Chang 2020; Jang and Yang 2023). Both parameters are influenced by porosity, tortuosity, and water/cement ratio, with excessive carbonation reducing effective diffusivity through pore network changes. When calculating apparent diffusivity, one must consider the qualities of the bulk material as well as the surrounding conditions to determine the total rate at which CO_2 diffuses through concrete (Yoon and Chang, 2020). Conversely, effective diffusivity is a more intrinsic metric parameter that considers the pore structure of the

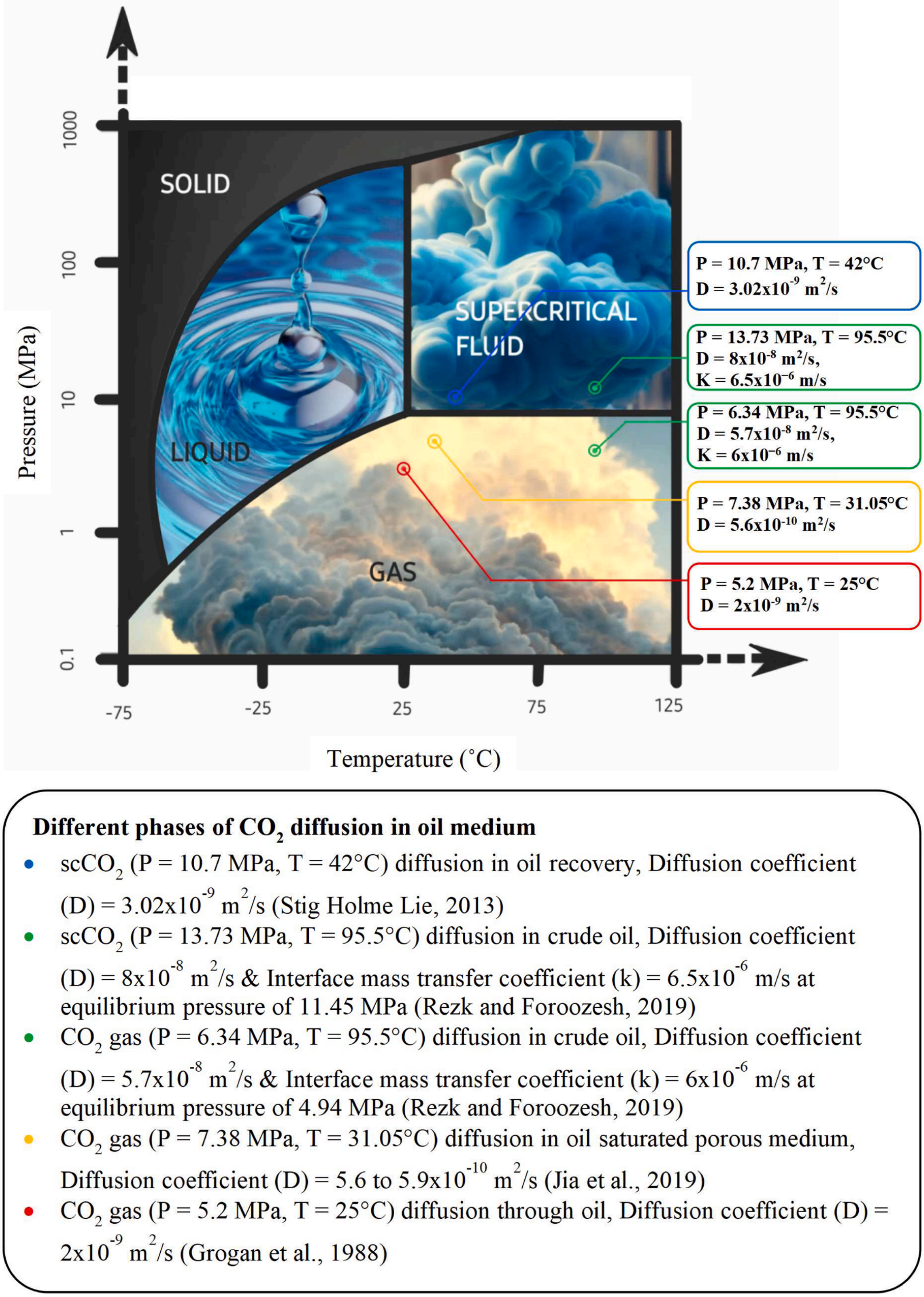

Different phases of CO_2 diffusion in oil medium

- ● $scCO_2$ (P = 10.7 MPa, T = 42°C) diffusion in oil recovery, Diffusion coefficient (D) = 3.02×10^{-9} m^2/s (Stig Holme Lie, 2013)
- ● $scCO_2$ (P = 13.73 MPa, T = 95.5°C) diffusion in crude oil, Diffusion coefficient (D) = 8×10^{-8} m^2/s & Interface mass transfer coefficient (k) = 6.5×10^{-6} m/s at equilibrium pressure of 11.45 MPa (Rezk and Foroozesh, 2019)
- ● CO_2 gas (P = 6.34 MPa, T = 95.5°C) diffusion in crude oil, Diffusion coefficient (D) = 5.7×10^{-8} m^2/s & Interface mass transfer coefficient (k) = 6×10^{-6} m/s at equilibrium pressure of 4.94 MPa (Rezk and Foroozesh, 2019)
- ● CO_2 gas (P = 7.38 MPa, T = 31.05°C) diffusion in oil saturated porous medium, Diffusion coefficient (D) = 5.6 to 5.9×10^{-10} m^2/s (Jia et al., 2019)
- ● CO_2 gas (P = 5.2 MPa, T = 25°C) diffusion through oil, Diffusion coefficient (D) = 2×10^{-9} m^2/s (Grogan et al., 1988)

Fig. 5. Conceptual figure showcasing the various phases of CO_2 for diffusing CO_2 in a porous medium.

concrete as well as the pathways that allow CO_2 to diffuse (Jang and Yang, 2023). Since effective diffusivity ignores the impact of bulk characteristics and concentrates on diffusion via the actual pore network, it is usually lower than apparent diffusivity (Yoon and Chang, 2020).

3.3.2. *CO_2 phases and effects on diffusion*

CO_2 can be introduced into concrete in both gaseous and dissolved forms, with its diffusion influenced by the interaction between solutes and the porous cementitious matrix (Rezk et al. 2021). Unlike bulk liquid diffusion, molecular diffusion in porous media is constrained by the heterogeneous structure, which lengthens the travel path of solute

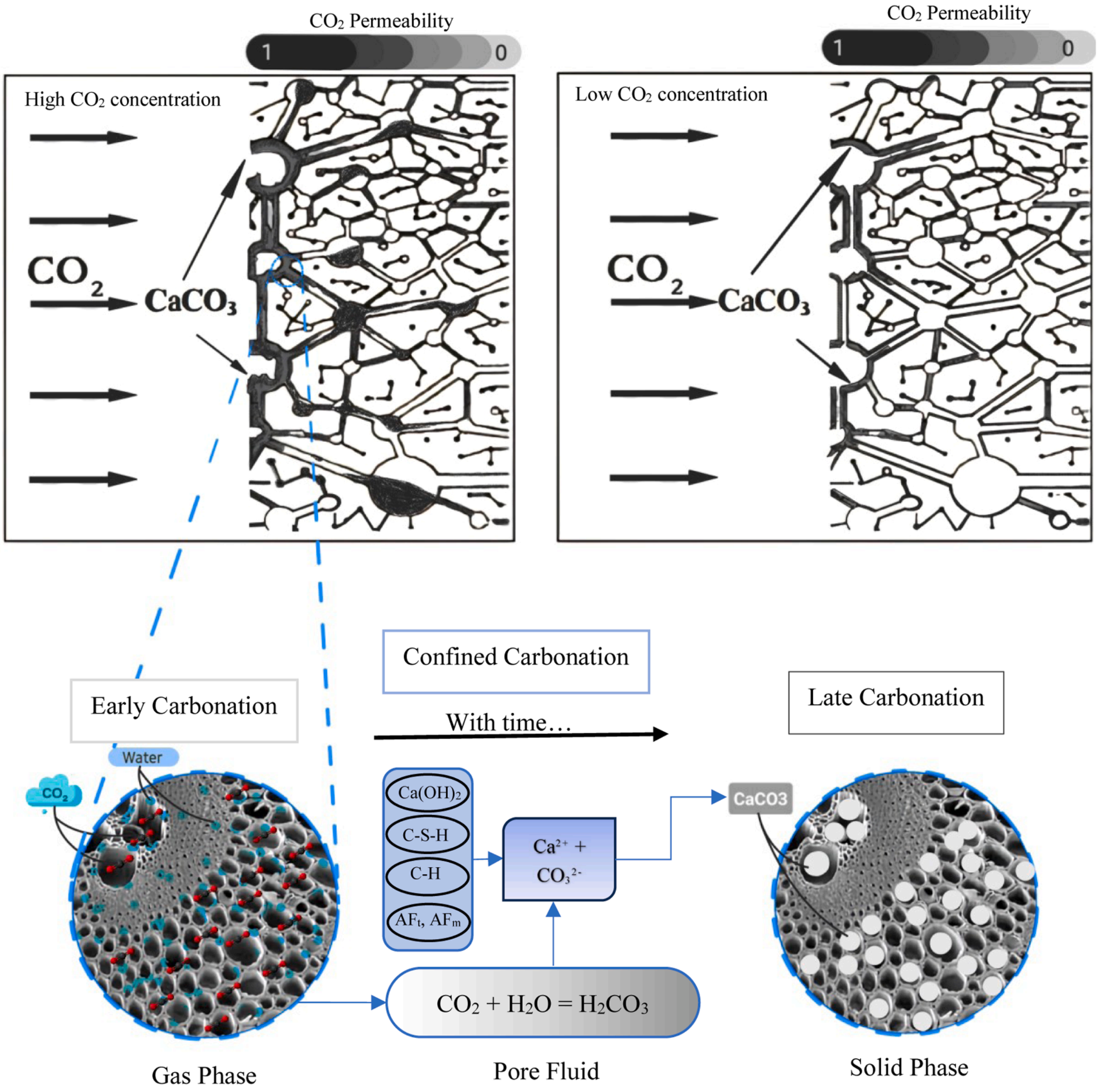

Fig. 6. Conceptual diagram indicating biochar's role in carbonation curing under high and low atmospheric CO_2 concentration.

molecules and reduces the effective diffusion coefficient (Lou et al. 2020).

CO_2 exists in four phases—solid, liquid, gas, and supercritical fluid—depending on temperature and pressure conditions (Clifford and Williams 2000). Fig. 5 shows a schematic representation of these phases and the diffusion in a porous medium with the variation in temperature and pressure, comparing findings from different studies. Among these, supercritical CO_2 ($scCO_2$), achieved at 30.85 °C and 74 bar, combines properties of both gas and liquid, offering unique diffusion characteristics (Rezk and Foroozesh 2019). Nikolai et al. 2019, conducted a thorough analysis of the thermodynamic and transport characteristics of $scCO_2$ containing binary mixtures, $scCO_2$+solute. It was observed that the thermodynamic state of CO_2 has a major impact on the mass transfer rate of CO_2. Rezk and Foroozesh (2019) found that in hydrocarbon-saturated porous media, $scCO_2$ exhibited higher diffusion coefficients (D) and mass transfer rates (K) than gaseous CO_2. For instance, oil swelling reached 30 % in 2 h with $scCO_2$ versus 10 h with gaseous CO_2, while viscosity reductions were 58 % and 25 %, respectively, over comparable durations. Li et al. (2016) also reported an order-of-magnitude increase in diffusion coefficients for $scCO_2$ compared to other phases. Jia et al. (2019) highlighted that the molecular diffusion coefficient depends heavily on the pressure and temperature of the medium. In heterogeneous systems, the porous matrix structure and composition significantly lower the diffusion coefficient relative to bulk liquid diffusion, adding complexity to CO_2 transport.

4. Biochar effects on carbon sequestration

4.1. CO₂ adsorption mechanism and effects of biochar

There are mainly two categories of adsorption. The first category is the physical adsorption of CO_2 molecules by the van der Waals force, which generally has a bond energy of 8–41 kcal/mol. Physical adsorption accounts for the majority of CO_2 adsorption in biochar. This includes interactions between adsorbed molecules, the biochar's abundant functional group arrangement, the traction effect created by the net charge exchange between the molecules and the metal ions, and the van der Waals force between the molecules (Zhang et al., 2022). Biochar typically contains oxygen-containing functional groups, such as hydroxyl (-OH), carboxyl (-COOH), and carbonyl (C = O) groups, distributed across its surface. These functional groups are primarily located on the edges and defects of the aromatic carbon structure and play a critical role in adsorptive interactions by providing active sites for chemical bonding and charge exchange. The second category is chemical adsorption, which predominantly relies on intermolecular compound interaction (Sharma et al., 2021). Many mechanisms have been brought

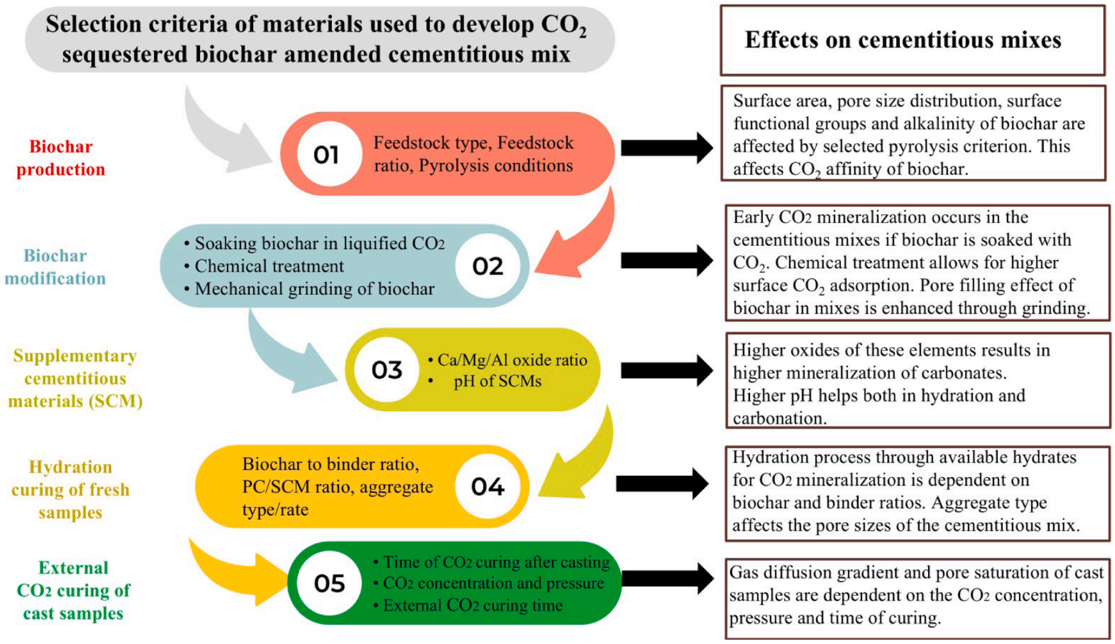

Fig. 7. Selection criteria for aiding carbonation and hydration curing in biochar-aided cementitious composites.

up to govern the process of CO_2 adsorption by biochar. Fig. A1 shows a schematic representation of the general CO_2 capture mechanism of biochar, such as cation exchange, precipitation, electrostatic attraction, reduction, and complexation (Shafawi et al., 2021). As per Zhang et al. 2020**,** the primary processes of CO_2 adsorption are complexation with functional groups; cation exchange with the surface of biochar; precipitation and formation of insoluble species; electrostatic attraction on the surface of biochar; reduction and further sorption of reduced compounds. These processes are generally dependent on the feedstock type, as biochar with different feedstock will likely show relatively different adsorption mechanisms. For example, large concentrations of phosphate and carbonate can be seen in manure biochar (Poucke et al. 2019). When biochar has a high concentration of calcium, potassium, magnesium, and sodium along with a reasonably high cation exchange capacity (CEC), cation exchange can be the predominant mechanism for CO_2 adsorption (Ngo et al., 2023). When it comes to biochar with low CEC (which most likely occurs due to a significant degree of organic matter decomposition), other mechanisms also tend to be crucial, such as specific surface area and porosity (Tomczyk et al. 2020).

The presence of biochar can influence the hydration of cement. Due to the high pH and high water-absorption characteristics of biochar, it can absorb water during concrete mixing (Gupta and Kua, 2018). Usually, the excess water present in the mixed concrete promotes the formation of pores/voids through evaporation/bleeding, thereby resulting in poor mechanical and durability properties of concrete (Gupta, Kua, and Tan Cynthia 2017; Kim et al. 2019). If biochar is present in the system, the saturated biochar particles function as "reservoirs," releasing some of the absorbed moisture into the matrix, which serves as nucleation sites for hydration reactions (Gupta and Kua, 2018; Praneeth et al. 2020). The enhanced hydration promotes more hydration products, which fill pores and densify the matrix, thereby improving the mechanical and durability performance of concrete. The water (absorbed by biochar) can be released during the hardening stage, leading to secondary hydration (and internal curing), which can also improve the performance of concrete as well as carbon sequestration (Choi, Yun, and Lee 2012). Replacement of cement with up to 2 % biochar did not significantly affect the hydration, but further substitution affected the hydration of cement as indicated by lower heat of hydration (Sikora et al. 2022).

The specific reactivity of the phases and the availability of CO_2 determine the reaction products in the mortar, which are dependent on the interaction of carbonation and hydration at any given time (Zajac et al. 2020). Kua and Tan 2023, proposed a mechanism that demonstrated how the presence of biochar can impact hydration as well as the carbonation of cement. Fig. 7 shows a graphical illustration indicating the role of biochar in carbonation curing under high and low atmospheric CO_2 concentrations. In the beginning, "early carbonation" is initiated, during which early phases present in cement react with CO_2 adsorbed in biochar pores. Cement hydration occurs simultaneously, and it is enhanced by the diffusion of free water out of the pores of biochar. With the passage of time: 1) "Confined carbonation" is initiated in biochar pores, leading to the formation of $CaCO_3$, C-S-H_{low}, and aluminosilicate gel: 2) Hydration reactions result in the formation of C-S-H_{high}, CH, Af_t and AF_m phases: 3) "Late carbonation reactions" which results in conversion of a fraction of C-S-H_{high} to C-S-H_{low} . Carbonation barriers may be formed during this period, which restricts the flow of internal CO_2 as well as the flow of CO_2 from outside (Kua and Tan 2023). For instance, Zuo et al. 2024, observed that ACC up to 72 h resulted in higher values of carbon sequestration in concrete, but prolonged treatment exceeding 72 h affected carbon sequestration negatively. This is mainly attributed to two main factors. Firstly, prolonged exposure to CO_2 reduces the amount of reactive chemicals available for controlled CO_2 conditioning, which in turn reduces the specimens' ability to sequester CO_2. Secondly, to create carbonic acid (which is an essential step for the production of $CaCO_3$), CO_2 must dissolve in pore water. Even though biochar helps in depleting excess pore water during late hydration, extended carbonation depletes the free water, leaving insufficient water to facilitate further carbonation reaction.

4.2. Strategies for biochar development

Apart from the discussed mechanisms of biochar itself for CO_2 curing, the possible strategies by which biochar can affect carbonation and hydration curing in cementitious materials is discussed in this section. Overall, these strategies include biochar production methods, internal CO_2 doping in biochar, carbonation conditions, etc. All these strategies are likely to enhance either hydration curing or CO_2 curing. Fig. 6 shows a simplistic selection criterion for biochar usage in affecting hydration and carbonation in cementitious materials.

4.2.1. Biochar production and internal modifications

The feedstock used to produce biochar can impact its properties and CO_2 capture ability. The distribution of pores in biochar is influenced by the feedstock (Brewer et al. 2014). A higher carbon content in the feedstock suggests an increased potential for CO_2 sequestration (Gupta and Kua, 2017). The quality of biochar blocks is influenced by the type of feedstock used. Cross and Sohi (2013) discovered that, even at similar temperatures, biochar blocks made from sugarcane trash exhibited high stability, whereas those made from chicken manure were the least stable. Biochar with high stability has less tendency to be involved in harmful chemical reactions during cement hydration (Brewer et al. 2014). Pyrolysis conditions like temperature, pressure, and heating rate can significantly influence the surface area of the biochar formed (Brownsort 2009; Munroe 2009; Sohi et al. 2010). Pyrolysis temperature can influence many properties of biochar, including its stability, elemental composition, surface area, surface functional groups, etc. (Sun et al. 2014; Yuan et al. 2014). As pyrolysis temperature increases, the carbon content of biochar increases while its oxygen, nitrogen, and hydrogen contents decrease (Zhang, Liu, and Liu 2015). In the case of rubber wood saw dust, increasing the pyrolysis temperature from 300 to 500 °C did not increase surface area, whereas raising the temperature to 700 °C led to significant increases in surface area (Shaaban et al. 2013). In the case of safflower seed press cake, there was an increase in surface area as the temperature was increased up to 500 °C, while surface area decreased as temperature exceeded 500 °C, possibly due to pore widening, neighbouring pore coalescence, softening, and melting (Angın 2013). At high pyrolysis temperatures, secondary reactions occur in biochar, leading to a reduction in the final amount of biochar produced (while proportions of biogas and bio-oil increase) (Antal and Grønli 2003; Boateng 2007). When the pyrolysis temperature is high, it leads to less reactive sites and, hence, higher biochar stability (Gupta and Kua 2017). Fast pyrolysis (heating rate = 100–1000 °C/s & shorter residence time) leads to a lower amount of biochar, while slow pyrolysis (heating rate = 10 °C/s & longer residence time) leads to a higher amount of biochar as vapor production during secondary reactions decreases (Gupta and Kua 2017). Fast pyrolysis has been reported to produce biochar with high surface area, higher oxygen, and lower carbon content when compared to slow pyrolysis (Bruun et al. 2012). The size of biochar particles produced during fast pyrolysis is roughly five times smaller when compared to slow pyrolysis. Lower residence time can lead to reduced micropore volume and surface area (Gupta and Kua 2017). The influence of residence time on biochar properties is not straightforward, as biochar properties are often dominated by other synthesis parameters (Fassinou et al. 2009). Biochar produced at 30 bar pressure exhibited less cavity and denser structure when compared to biochar produced at 1 bar pressure (Okumura, Hanaoka, and Sakanishi 2009). The surface area of biochar is reduced as pressure is raised from 5 to 10 bar, while it increases with an increase in pressure from 10 to 20 bar (Newalkar et al. 2014). As the pressure is increased, biochar particles are more spherical in shape (Newalkar et al. 2014).

It was reported that the surface area of biochar may not correlate with its CO_2 capture ability (Brewer et al. 2014) as the surface area is also affected by macropores and mesopores. Knowledge of pore size distribution is needed because CO_2 capture is optimized when pores are in a certain range (<2 nm) (Brewer et al. 2014). To increase the selective adsorption of CO_2, the isosteric heat of adsorption of CO_2 on the pores must be higher than that of other gases (Park and Suh 2013). Isosteric heat of CO_2 adsorption will be high when the pore size distribution is close to the diameter of CO_2 molecules. Higher CO_2 adsorption is obtained when the pore size is between 0.33 and 0.82 nm (Hu et al. 2011; Presser et al. 2011; Sevilla and Fuertes 2011).

Biochar has a CO_2 reduction potential of around 870 kg CO_2 equivalent per ton of dry feedstock (Roberts et al. 2010). However, if biochar is pre-exposed to CO_2 before its use for construction, it can additionally capture 300 kg CO_2 equivalent per ton of dry feedstock (Wei et al. 2012). This is called pre-cured CO_2 sequestration in biochar. Biochar can be activated physically or chemically to improve its CO_2 absorption capacity as it increases its pore volume and surface area (Schröder et al. 2007). Physical activation involves oxidizing agents like CO_2, steam, or both (Rodriguez-Reinoso et al., 1995). The CO_2 activation is accomplished by the carbon-CO_2 reaction, leading to burn off carbon atoms, thereby opening closed pores as well as widening existing pores (Rodríguez-Reinoso and Molina-Sabio 1992).

Activation of biochar with steam leads to the release of volatile components and enhanced formation of crystalline carbon components (Alaya, Girgis, and Mourad 2000). Chemical activation involves the treatment of biochar with chemicals like NaOH, KOH, ZnCl, etc. (Pimentel et al., 2023). During chemical activation, chemicals dehydrate biochar and then wash off volatile compounds, leading to higher carbonization yield (Williams and Reed 2004). Overall pore volume and surface area increase with an increase in activation temperature and chemical agent (KOH) to biochar ratio (Sevilla and Fuertes 2011). Temperature and duration of activation must be optimized to maximize the CO_2 adsorption (Wei et al. 2012). At higher temperatures, the adsorption of CO_2 can decrease due to reduced pore filling (Wei et al. 2012). Internal CO_2 doping of dry biochar may lead to mortar (which incorporated it) possessing high mechanical strength as well as high CO_2 absorption when compared to the mortar produced with dry biochar without internal CO_2 doping (Kua and Tan 2023). Internal curing of biochar improved the carbonation of steel slag-based artificial lightweight aggregates by providing additional channels for diffusion as well as biochar acting as a temporary CO_2 storage tank (Xu et al. 2023), resulting in improved performance of concrete. The activation of biochar with low oxygen concentration has been found to result in the formation of micropores capable of capturing CO_2 in ambient conditions (Plaza et al. 2014).

4.2.2. Surface modifications

The introduction of functional groups on the biochar surface can improve its CO_2 adsorption capacity. Modifications with ammonia have been found to increase the surface alkalinity of biochar through the incorporation of compounds containing nitrogen, and this has resulted in an enhanced affinity of biochar for CO_2 (Xiong et al. 2013). However, if the modifying temperature is high, ammonia modification is not efficient, possibly because of the decomposition of the attached nitrogen-containing groups and the collapse of the porous structure (Han et al., 2021). It is reported that biochar modified with CO_2 exhibited higher CO_2 adsorption capacity at ambient temperatures, while biochar modified with ammonia performed well at high temperatures (Jansen and van Bekkum 1994; Shafeeyan et al. 2011). In the case of the performance of biochar treated with ammonia and biochar subjected to peroxidation before ammonia treatment, CO_2 adsorption was observed to be higher in the former than in the latter (Shafeeyan et al. 2011). The presence of amine and pyridine groups on the surface of biochar can improve its CO_2 adsorption capacity (Shafeeyan et al. 2011); however, regeneration of adsorbed CO_2 may be difficult because chemical bonding between adsorbed CO_2 and the functional group is stronger (Raganati et al. 2021). In the case of low-temperature adsorption, it is possible that amine groups block the micropores of biochar and, hence, lower the surface area and CO_2 adsorption capacity (Madzaki and KarimGhani, 2016).

4.3. Application of biochar in curing processes

Hydration curing of biochar depends on various factors like biochar to binder ratio, OPC/SCM ratio, SCM type, aggregate type, etc. It can be observed from Table A2 that by adding other binders like Fly ash, slag, sand, superplasticizers, etc., with biochar, the CO_2 uptake can be further enhanced (Praneeth et al. 2020; Liu et al. 2023; Mishra et al. 2023a). Mishra et al. (2023a) found that after 3 days of CO_2 curing, 1 % biochar concrete was able to uptake 5.3 % CO_2 by mass, while just by adding 1 % class C fly ash to the mix 6 % CO_2 uptake was seen. And further, by adding 1 % nanosilica instead of fly ash, the CO_2 uptake was 7.2 % by mass. On the other hand, Praneeth et al. 2020, didn't find any significant increase in CO_2 uptake after 3 days of CO_2 curing when comparing 2 %, 4 %, 6 %, and 8 % biochar mixed with different percentages of fly ash. It was also seen that mixing more biochar doesn't always increase the CO_2 uptake, as is evident from Table A3. By mixing 4 % biochar, Praneeth et al. (2020) demonstrated that the CO_2 uptake increased up to 13 %, but when 6 % and 8 % biochar were mixed, CO_2 uptake was only 11.3 % in both cases (Praneeth et al. 2020). Nevertheless, it is evident from these studies that it is possible to increase the amount of CO_2 mineralisation by optimizing the hydration process with the help of SCMs.

Table A3 indicates how adding biochar during accelerated carbonation can greatly improve CO_2 uptake, especially when using larger amounts of biochar. For instance, Agarwal et al. (2023) found that just by adding 5 % biochar, the CO_2 uptake after 4 h curing was increased by 4.5 percentage points when compared to normal concrete. The time of exposure, desaturation of blocks, CO_2 concentration, and pressure all play an important role in external CO_2 curing, which affects the overall CO_2 mineralisation. As the CO_2 concentration increases, CO_2 diffusion in the concrete matrix also increases initially, but as more and more pore spaces on the surface get filled, the rate of diffusion decreases with time (Cui et al. 2015). Agarwal et al. (2023) found that just after 4 h of accelerated CO_2 curing, the maximum CO_2 uptake for 5 % biochar concrete went up to 11 %, but in the case of Praneeth et al. 2020 with 4 % biochar concrete, the maximum CO_2 uptake even after 3-days of CO_2 curing was only 13 %.

4.4. *Impact on material properties*

4.4.1. *Thermogravimetric analysis*

Thermogravimetric analysis (TGA) and differential thermogravimetric analysis (DTG) have been emplyed to study the carbonation behaviour biochar amended cementitious composites. Literature in Table A1 indicate that biochar addition significantly impacts weight loss patterns, indicating changes in hydration and carbonation products. Five intervals can be identified in the decomposition of cementitious composites: I (40–100 °C) is associated with C–S–H and ettringite; II (100–200 °C) is associated with AF_m; III (350–500 °C) is associated with the portlandite; and IV (600–700 °C) and V (700–800 °C) are associated with carbonates, (predominantly by $CaCO_3$). Because of its porous structure and large surface area, biochar facilitates the hydration reaction and improves the efficiency of the CO_2 reaction. This increases the decomposition peaks in intervals I, II, and III for samples blended with biochar (Liu et al. 2023).

The TGA/DTGA analysis also indicates that especially after 28 days curing, carbonation of biochar-blended composites causes a decrease in hydration product decomposition peaks and an increase in carbonate decomposition peaks (Liu et al., 2023; Mishra et al. 2023). Yang and Wang (2021) discovered that mortar blended with biochar displayed a higher degree of carbonation and increased $CaCO_3$ content, which facilitated ACC. While Agarwal et al. (2023) observed that biochar-enriched mixes accelerated the carbonation process and increased mineralization of $CaCO_3$ compared to plain OPC mixes, Wang et al. (2021) reported that biochar-modified samples exhibited larger peaks of CH, suggesting a significant promotion of cement hydration. The combination of fly ash and biochar has a synergistic impact that increases the degree of internal carbonation, modifies the polymorph composition of $CaCO_3$, and increases the overall carbonation efficiency.

4.4.2. *Mechanical properties*

Table A2. compiles recent studies done on biochar usage in concrete or cementitious rigid bodies. The table catalogues the Portland cement percentage used, the biochar (whether treated or untreated) application rate, ACC conditions, the SCM types and rate, and the observed long and short-term compressive strength of the composites. It is observed that the effect of biochar on mechanical properties in cementitious composites is largely dependent on the OPC amount, biochar amount used, and curing conditions. For instance, when OPC was used >50 %, the short-term strength (i.e., 7 days) increased up to 3 % and 22 % (Praneeth et al. 2020). The improvement in early-age strength is attributed to the porous structure and large surface area of biochar, which enhance the hydration reactions. Similar observations have been reported in Agarwal et al. (2023), with reported short-term (7 days) and long-term (28 days) strength increasing by up to 40 % and 32 %, respectively. It was noticed that adding as little as 1 % biochar to concrete blocks that were cured with 100 % CO_2 at 1.1 bar for 24 h increased the short-term compressive strength of the concrete blocks by 71 % (Wang et al. 2020). The favourable positive strength results for Agarwal et al. (2023) are attributed to continuous ACC for the entire curing period, while Praneeth et al. (2020) only applied for 2 h. Mishra et al. (2023a) and Wang et al. (2021) did not find considerable increase in compressive strength at higher OPC usage ($\geq$ 50 %). Nevertheless, the benefits of biochar and ACC are reflected at lower OPC addition with other SCMs being used (T. Chen et al. 2022; Yang and Wang 2021; Kua and Tan 2023).

The particle size of biochar significantly influences the mechanical properties of cementitious materials. A mix of 1:1 ratio of coarse-grained and fine-grained biochar works better than single-size particles. Since finer and coarser biochar have a synergistic impact and a higher surface area, the combination of the two can improve the degree of hydration of cement by 6–12 % compared to using only coarse biochar (Gupta et al. 2021). Biochar made from plant-based feedstocks (at 450 °C slow pyrolysis rate) increased the 28-day compressive strength of OPC composites by 3–13 % (Z. Zhao et al. 2024). Compressive strength is further increased by 2–7 % by adding biochar with smaller particle sizes (added at <2.5 % of the binder weight). It does, however, also point out that the addition of fine and coarse materials, such as sand and gravel, might counteract these positive benefits, sometimes making the impact of the biochar on compressive strength insignificant (L. Zhao et al. 2024). However, the optimal combination of curing conditions and the quantity of biochar impacts the strength significantly. While biochar additions increased compressive strength in some mixtures, the outcomes differed based on the conditions and materials employed. For instance, adding 5 % biochar to a cement mixture containing 40 % fly ash and curing it in CO_2 resulted in a 40 % increase in compressive strength (Xu et al. 2023). At higher biochar content (above 5 %), a trend in decreasing strength was observed (Praneeth et al. 2020; Agarwal et al. 2023). This is mainly due to the accumulation of biochar particles hindering the formation of a dense and continuous matrix, which leads to the formation of micropores and microcracks within the concrete matrix. The foregoing discussion reveals that there is no direct established methodology that showcases optimum biochar and OPC ratio that would give higher strength. Nevertheless, if CO_2 mineralization is of priority and strength requirements are low, these kinds of rigid cementitious materials can still be used as Low-Strength Concrete Blocks (Category C3) as per Eurocode 6 (EN 1996) provisions (Liu et al. 2023).

5. Present gap areas for future research

The future research areas, based on the current gaps discussed in the previous sections, are detailed below in four categories.

5.1. *Conditions for CO_2 diffusion in biochar-amended cementitious materials*

A promising area for faster CO_2 sequestration in biochar-amended cementitious materials lies in exploring different phases of CO_2, particularly $scCO_2$, as opposed to traditional gaseous CO_2. While $scCO_2$ has demonstrated a faster diffusion rate in the case of hydrocarbon-based porous materials, similar evidence is lacking in cementitious composites. Additionally, there is scope for utilizing negative pressure, that can facilitate rapid CO_2 diffusion into the cementitious pore matrix

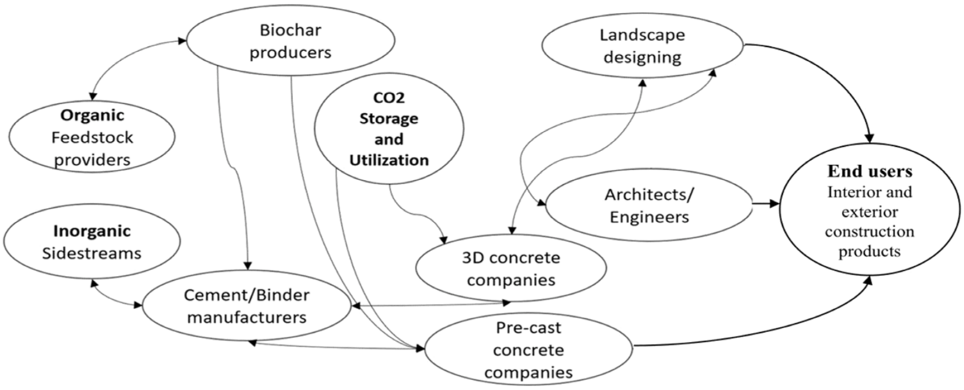

Fig. 8. Value chain of industries that would be impacted by the mainstream commercialization of biochar in CO_2-sequestered cementitious composites.

(Dixit et al. 2021). Another alternative is to reduce moisture before carbonation like those observed by Hanafi et al. (2024). Utilization of cold bonded aggregates (Tajra et al. 2019) in concrete blocks may offer a more efficient approach to CO_2 sequestration without pore blockage problems.

5.2. Design of specialised biochar for CO_2 mineralization

The use of different pyrolysis conditions, such as temperature and residence time, can greatly alter the surface morphology, honeycomb structure, and aromaticity, which alters CO_2 mineralization and hydration kinetics (Pariyar et al. 2020). Alternatively, to reduce the heterogeneity of the feedstock observed in the literature (Das et al. 2021), one can adopt gas pyrolysis, such as methane, to produce homogenous biochar-like materials. Another promising strategy involves pre-soaking biochar in different forms of CO_2, such as carbonic acid or chemically absorbed CO_2, to further improve its effectiveness in the CO_2 mineralization processes (Kua and Tan 2023). Adding calcium or magnesium nanoparticles to biochar could potentially improve their ability to mineralize CO_2.

5.3. Engineering assessment of durability characteristic

As Table A2 illustrates, most recent studies have been on evaluating the short-term compressive strength of cementitious materials treated with biochar. However, these materials' anticipated lifespan in the building industry varies from 10 to 100 years; thus, a thorough assessment of their long-term durability is required. The existing literature noticeably lacks important evaluations, including leaching behaviour and freeze-thaw resistance. The leaching potential of metals at the end of the life cycle of these materials is hitherto neglected in current literature emphasising the need to investigate the aspect. It is most likely that as biochar has high adsorption potential, the demolished waste can still be used as an adsorbent and would not leach out harmful contaminants from leachable SCMs such as fly ash, slag, and tailings (Jhatial et al. 2023). A proper leaching assessment should consider conditions of extreme pH and liquid-to-solid ratio as per USEPA regulations (L. Zhao et al. 2024). Freeze-thaw resistance is of particular concern in cold regions such as the Nordics, Canada, and parts of Northern America. As biochar is highly hydrophilic, it is probable that it may retain moisture and exacerbate the freezing-thawing-related damages in cementitious material.

5.4. Development of compatible SCMs

To reduce overall CO_2 emission in biochar-amended cementitious composites, the relevance of utilizing SCMs can be seen in Table A2 and A3. The SCMs can be further improved in such a way that the utilization of cement can be further reduced and the SCMs on itself can help in CO_2 mineralization as well as the hydration reaction. Fig. A2 gives a visual representation of different treatments that can enhance the hydration and CO_2 mineralization of SCMs. For instance, after segregation, the finer fractions of mine tailing or slag seem to get more evenly distributed in the concrete matrix, which results in better reactivity, ensuring consistent hydration and carbonation (Power et al. 2021). SCMs like natural pozzolans and ferrous slag can be grounded to a specific surface area, which enhances their reactivity during hydration and carbonation (Lemonis et al. 2015). In the case of incineration ash, recycled concrete, bio-fibers, etc., wet chemical treatment can potentially change the surface oxide distributions, remove impurities, and increase the reactivity of the materials (Langley et al. 2007). Some SCMs, like calcined clays, can have higher reactivity towards CO_2. This activation increases their reactivity when mixed with cement, improving the strength and durability of the resulting concrete (Bullerjahn et al. 2020).

6. Concluding remarks

Recent efforts to reduce CO_2 emissions in the concrete sector have focused on biochar-amended cementitious materials. This review emphasises how, when properly managed and integrated, biochar has a significant potential to lower total CO_2 emissions in the built environment. However, as mentioned throughout the review, many gap areas still need to be addressed before they can be utilised as a conventional construction material. Some salient concluding statements are made below.

- There is a need to develop uniform biochar so that these materials can be utilized in a standardised form in the construction sector.
- It is observed that the mechanisms to improve CO_2 diffusion are relatively lacking, at least from the point of view of use in cementitious material. The knowledge that exists from other hydrocarbon-based materials for CO_2 diffusion can be incorporated to better understand the diffusion mechanism in biochar-amended SCMs.
- As a value chain, there is still scope for optimization of various stakeholders that need to work together to develop the next generation of biochar-stabilized cementitious composites. A conceptual value chain map for the stakeholders, starting from the raw material providers to the end users, is presented in Fig.8. The organic feedstock from the pulp industry, forest industry, municipal waste, etc., can be fractionated and used for biochar production. The produced biochar can then be utilized in both binder manufacturing and precast concrete manufacturing.

CRediT authorship contribution statement

Soumya Roy: Writing – review & editing, Investigation, Data curation. **Harisankar Sreenivasan:** Writing – review & editing, Data curation. **Ajit K Sarmah:** Writing – review & editing. **Hossein Baniasadi:**

Writing – review & editing. **Sanandam Bordoloi:** Writing – original draft, Supervision, Funding acquisition, Conceptualization.

Declaration of competing interest

All authors have no conflict of interest in submission to “Resources, Conservation and Recycling”.

Acknowledgement

The last author acknowledges the support of FINNCERES flagship, and the startup tenure track fund (91160169 (TT/Bordoloi)) provided by Aalto University.

Appendix

Table A1
Properties measured on biochar-amended cementitious mixtures with accelerated CO_2 curing.

Reference	Location of research	Biochar (%by wt.)	CS	FS	TP	WA	F-T	Leaching	CO_2 uptake	UPV	Chloride diffusion	Heat of Hydration
Praneeth et al. 2020	New Zealand-China	0–8	√	×	√	√	×	×	√	×	×	×
Wang et al. 2020	Hong Kong	0–1	√	×	√	×	×	×	×	×	×	×
Yang and Wang.2021	Korea	0–5	√	×	√	×	×	×	×	√	√	×
Wang et al. 2021	Korea-Hong Kong	0–2	√	×	√	×	×	×	×	×	×	×
T. Chen et al. 2022	China	0–5 %	√	×	√	√	×	×	√	×	×	×
Liu et al. 2023	China	0–15	√	×	√	√	×	×	√	×	×	×
Mishra et al. 2023a	United States of America	0–1.5	√	√	√	×	×	×	√	×	×	√
Mishra et al. 2023b	United States of America	0–5	√	√	√	×	×	×	√	×	×	×
Kua and Tan 2023	Singapore	0–2	√	√	√	×	×	×	√	×	×	×
Xu et al. 2023	China	0–3	√	×	√	√	×	×	√	×	×	×
Agarwal et al. 2023	India	0–10	√	×	√	√	×	×	√	×	×	×
Wyrzykowski et al. 2024	Switzerland	0–8.5	√	×	×	×	×	×	×	×	×	×

*CS: Compressive strength; FS: Flexural strength; TP: Thermogravimetric properties; WA: Water absorption; F-T: Freeze-Thaw; UPV: Ultrasonic Pulse Velocity.

Table A2
Tabulated effect of biochar and accelerated carbonation on compressive strength of concrete blocks.

Reference	OPC (%by total solid wt.)	Biochar (BC) (% by wt.)	CO_2 BCE (% by wt.)	ACC procedure	SCMs or aggregates	Short-term (ST) (in MPa) *32 at 3 days*[#]	Final term (FT) (in MPa) NA
Praneeth et al. 2020	80	0	0	NC, AC	20 % FA	***32 at 3 days***[#]	NA
	79	2	0		19 % FA	33 at 3 days	NA
	78	4	0		18 % FA	33.5 at 3 days	NA
	77	6	0		17 % FA	29 at 3 days	NA
	76	8	0		16 % FA	25.5 at 3 days	NA
	80	0	0	100 % CO_2, 1 MPa, 2hr	20 % FA	33.5 at 3 days	NA
	79	2	0		19 % FA	35.3 at 3 days	NA
	78	4	0		18 % FA	40 at 3 days	NA
	77	6	0		17 % FA	39 at 3 days	NA
	76	8	0		16 % FA	35.5 at 3 days	NA
	60	0	0	NC, AC	40 %FA	***12.7 at 3 days***[#]	NA
	59	2	0		39 % FA	14.5 at 3 days	NA
	58	4	0		38 % FA	14.4 at 3 days	NA
	57	6	0		37 % FA	13.7 at 3 days	NA
	56	8	0		36 % FA	14 at 3 days	NA
	60	0	0	100 % CO_2, 1 MPa, 2hr	40 %FA	13 at 3 days	NA
	59	2	0		39 % FA	15.5 at 3 days	NA
	58	4	0		38 % FA	15.4 at 3 days	NA
	57	6	0		37 % FA	14.4 at 3 days	NA
	56	8	0		36 % FA	14.3 at 3 days	NA
	50	0	0	NC, AC	50 % FA	***12.5 at 3 days***[#]	NA
	49	2	0		49 % FA	13.2 at 3 days	NA
	48	4	0		48 % FA	13.5 at 3 days	NA
	47	6	0		47 % FA	11.6 at 3 days	NA
	46	8	0		46 % FA	13.8 at 3 days	NA
	50	0	0	100 % CO_2, 1 MPa, 2hr	50 % FA	15.4 at 3 days	NA
	49	2	0		49 % FA	17.5 at 3 days	NA
	48	4	0		48 % FA	17.5 at 3 days	NA
	47	6	0		47 % FA	15.4 at 3 days	NA
	46	8	0		46 % FA	17.6 at 3 days	NA

(*continued on next page*)

Table A2 (*continued*)

Reference	OPC (%by total solid wt.)	Biochar (BC) (% by wt.)	CO_2 BCE (% by wt.)	ACC procedure	SCMs or aggregates	Short-term (ST) (in MPa) 32 *at 3 days* #	Final term (FT) (in MPa) NA
Wang et al. 2020	50	0	0	NC, AC	50 % sand	***45 at 7 days*** #	NA
	50	1	0	NC, AC	49 % sand	48.5 at 7 days	NA
	50	0	1	100 % CO_2,1.1 bar, 24 h	49 % sand	51 at 7 days	NA
	50	1	0	100 % CO_2,1.1 bar, 24 h	49 % sand	77 at 7 days	NA
Yang and Wang.2021	100	0	0	60 % RH; 5 % CO_2, 0.1 MPa, 7 and 28 days	NA	***31.76 at 3 days*** #	***47.59 at 28 days*** #
	98	2	0		NA	31.34 at 3 days	44.76 at 28 days
	95	5	0		NA	25.8 at 3 days	41.77 at 28 days
	40	0	0		60 % Sand	32.87 at 3 days	60.83 at 28 days
	38.8	2	0		60 % Sand	32.1 at 3 days	58.23 at 28 days
	37.2	5	0		Sand	31.03 at 3 days	54.37 at 28 days
Wang et al. 2021	0	0	0	75 % RH;10 % CO_2, 1.1 MPa, 7 and 28 days	100 % Magnesia cement	***25.5 at 7 days*** #	***26 at 28 days*** #
	0	2	0		100 % Magnesia cement	20 at 7 days	27 at 28 days
	0	0	2		100 % Magnesia cement	24 at 7 days	28.5 at 28 days
	50	0	0		Magnesia cement	*26 at 7 days*	*30.5 at 28 days*
	49	2	0		Magnesia cement	28.5 at 7 days	32 at 28 days
	49	0	2		Magnesia cement	30 at 7 days	46.5 at 28 days
T. Chen et al. 2022	40		0	NC, AC	60 % Sand	19 at 3 days	30 at 28 days
	39	1	0	70 % RH @ 20 °C, 20 % CO_2, 1 MPa, 24h	60 % Sand	27.5 at 3 days	36.8 at 28
	37	3	0		60 % Sand	30 at 3 days	42 at 28 days
	35	5			60 % Sand	31 at 3 days	43.8 at 28
Liu et al. 2023	10	0	0	NC, AC	20 % GGBFS, 70 % BOFS	***8.46 at 7 days*** #	***8.67 at 28 days*** #
	10	5	0		15 % GGBFS, 70 % BOFS	6.03 at 7 days	7.29 at 28 days
	10	10	0		10 % GGBFS, 70 % BOFS	4.77 at 7 days	6.41 at 28 days
	10	15	0		5 % GGBFS, 70 % BOFS	4.24 at 7 days	5.20 at 28 days
	10	0	0	CO_2 under 1 atm, 72 h	20 % GGBFS, 70 % BOFS	7.67 at 7 days	7.58 at 28 days
	10	5	0		15 % GGBFS, 70 % BOFS	5.72 at 7 days	6.55 at 28 days
	10	10	0		10 % GGBFS, 70 % BOFS	5.92 at 7 days	6 at 28 days
	10	15	0		5 % GGBFS, 70 % BOFS	8.49 at 7 days	6.87* at 28 days
Mishra et al. (2023a)	100	0	0	3 days AC, 12 % CO_2, 65 %RH, 1.02 atm, 7 days	NA	***25.81 at 7 days*** #	NA
	99	1	0		NA	25.97 at 7 days	NA
	88.9	1	0		1 % Class C FA	25.14 at 7 days	NA
	98	1	0		1 % Nano Silica	26.03 at 7 days	NA
Mishra et al. (2023b)	100	0	0	3 days AC, 12 % CO_2, 65 %RH, 1.02 atm, 7 days	0	*26.47 at 7 days*	*29.52 at 28 days*
	90	0	0		10 %FA	24 at 7 days	27.5 at 28 days
	87.5	2.5	0		10 %FA	26 at 7 days	27 at 28 days
	85	5	0		10 %FA	20 at 7 days	28 at 28 days
	75	0	0		25 %FA	23 at 7 days	33 at 28 days
	72.5	2.5	0		25 %FA	22 at 7 days	29 at 28 days
	70	5	0		25 %FA	21 at 7 days	29 at 28 days
	60	0	0		40 %FA	26.9 at 7 days	38 at 28 days
	57.5	2.5	0		40 %FA	24 at 7 days	32 at 28 days
	55	5	0		40 %FA	20 at 7 days	30 at 28 days
Kua and Tan (2023)	29.2	0	0	NC, AC	70.5 % Sand, 0.3 % super plasticizer	NA	***50 at 28 days*** #
	29.2	0	0	0.5 % CO_2, 1 atm, 48 h, AC	70.5 % Sand, 0.3 % super plasticizer	NA	53 at 28 days
	29.2	1	0		70.5 % Sand, 0.3 % super plasticizer	NA	58.5 at 28 days
	29.2	0	1	99.9 % CO_2, 48 h, EC	70.5 % Sand, 0.3 % super plasticizer	NA	55.5 at 28 days
	29.2	1	0	EC	70.5 % Sand, 0.3 % super plasticizer	NA	46 at 28 days
	29.2	0	1	BC, EC	70.5 % Sand, 0.3 % super plasticizer	NA	46 at 28 days
	29.2	1 (PS)	0	NC, AC	70.5 % Sand, 0.3 % super plasticizer	NA	48 at 28 days

(*continued on next page*)

Table A2 (*continued*)

Reference	OPC (%by total solid wt.)	Biochar (BC) (% by wt.)	CO_2 BCE (% by wt.)	ACC procedure	SCMs or aggregates	Short-term (ST) (in MPa)	Final term (FT) (in MPa)
						32 at 3 days #	NA
	29.2	0	1 (PS)	BC, NC	70.5 % Sand, 0.3 % super plasticizer	NA	48.2 at 28 days
	29.2	1 (PS)	0	EC	70.5 % Sand, 0.3 % super plasticizer	NA	53 at 28 days
	29.2	1	1 (PS)	BC, EC	70.5 % Sand, 0.3 % super plasticizer	NA	48 at 28 days
Xu et al. (2023)	18.8	0	0	60 % RH; 99.9 % CO_2, 0.2 MPa, 4 h	Natural limestone aggregate	***30 at 3 days*** #	***43 at 28 days*** #
	18	0	0		39 % SS, 7.3 % FA, CA	23 at 3 days	30 at 28 days
	18.75	0.45	0		37.5 % SS, 7 %FA, CA	27.5 at 3 days	36 at 28 days
	19.2	1	0		36.3 % SS, 6.8 % FA, CA	29 at 3 days	38.5 at 28 days
	19.7	2	0		35.1 % SS, 6.6 % FA, CA	23 at 3 days	32.5 at 28 days
	20.3	2.96	0		33.8 % SS, 6.3 % FA, CA	21.5 at 3 days	28 at 28 days
Agarwal et al. 2023	100	0	0	75 % RH;10 % CO_2, 7 and 28 days	NA	***30 at 7 days*** #	***34 at 28 days*** #
	97	3	0		NA	33 at 7 days	43 at 28 days
	95	5	0		NA	42 at 7 days	45 at 28 days
	90	10	0		NA	23 at 7 days	26.5 at 28 days

*PS: Pre-soaked, SS: Steel slag, FA: Fly ash, CA: Cement aggregate, AC: Air curing, BC: Biochar curing, EC: External curing, NC: No curing, RH: Relative humidity, GGBFS: Ground Granular Blast Furnace Slag, BOFS: Blast Oxygen Furnace Slag.

Table A3

Tabulated effect of biochar and accelerated carbonation on CO_2 uptake.

Reference	**OPC (%by total solid wt.)**	**Biochar (BC) (%by wt.)**	**CO_2 BCE (%by wt.)**	**Other major binders**	**CO_2 uptake at any time**
Praneeth et al. 2020	80	0	0	20 % FA	12.4 % in mass (3 days)
	79	2	0	19 % FA	12.8 % in mass (3 days)
	78	4	0	18 % FA	13 % in mass (3 days)
	77	6	0	17 % FA	11.3 % in mass (3 days)
	76	8	0	16 % FA	11.3 % in mass (3 days)
	60	0	0	40 %FA	8.5 % in mass (3 days)
	59	2	0	39 % FA	9 % in mass (3 days)
	58	4	0	38 % FA	9 % in mass (3 days)
	57	6	0	37 % FA	10.3 % in mass (3 days)
	56	8	0	36 % FA	9.3 % in mass (3 days)
	50	0	0	50 % FA	8.8 % in mass (3 days)
	49	2	0	49 % FA	8.8 % in mass (3 days)
	48	4	0	48 % FA	9.3 % in mass (3 days)
	47	6	0	47 % FA	8.3 % in mass (3 days)
	46	8	0	46 % FA	8.8 % in mass (3 days)
Liu et al. 2023	10	0	0	20 % GGBFS, 70 % BOFS	0.64 g (28 days)
	10	5	0	15 % GGBFS, 70 % BOFS	1.01 g (28 days)
	10	10	0	10 % GGBFS, 70 % BOFS	1.48 g (28 days)
	10	15	0	5 % GGBFS, 70 % BOFS	2.64 g (28 days)
Mishra et al. (2023a)	100	0	0	NA	4 % in mass (3 days)
	99	1	0	NA	5.3 % in mass (3 days)
	88.9	1	0	1 % Class C FA	6 % in mass (3 days)
	98	1	0	1 % Nano Silica	7.2 % in mass (3 days)
Kua and Tan (2023)	29.2	0	0	70.5 % Sand, 0.3 % super plasticizer	NA
	29.2	0	0	70.5 % Sand, 0.3 % super plasticizer	0.46 % (28 days)
	29.2	1	0	70.5 % Sand, 0.3 % super plasticizer	0.91 % (28 days)
	29.2	0	1	70.5 % Sand, 0.3 % super plasticizer	1.33 % (28 days)
	29.2	1	0	70.5 % Sand, 0.3 % super plasticizer	1.64 % (28 days)
	29.2	0	1	70.5 % Sand, 0.3 % super plasticizer	2.36 % (28 days)
	29.2	1 (PS)	0	70.5 % Sand, 0.3 % super plasticizer	1.93 % (28 days)
	29.2	0	1 (PS)	70.5 % Sand, 0.3 % super plasticizer	2 % (28 days)
	29.2	1 (PS)	0	70.5 % Sand, 0.3 % super plasticizer	1.576 % (28 days)
	29.2	1	1 (PS)	70.5 % Sand, 0.3 % super plasticizer	2.94 % (28 days)
Xu et al. (2023)	18.8	0	0	Natural limestone aggregate	NA
	18	0	0	39 % Steel Slag (SS), 7.3 % Fly ash (FA), Cement aggregate (CA)	6.51 % (Sample Day NA)
	18.75	0.45	0	37.5 % SS, 7 %FA, CA	6.65 % (Sample Day NA)
	19.2	1	0	36.3 % SS, 6.8 % FA, CA	8.09 % (4 h)
	19.7	2	0	35.1 % SS, 6.6 % FA, CA	8.30 % (4 h)
	20.3	2.96	0	33.8 % SS, 6.3 % FA, CA	8.65 % (4 h)

(*continued on next page*)

Table A3 (*continued*)

Reference	OPC (%by total solid wt.)	Biochar (BC) (%by wt.)	CO_2 BCE (%by wt.)	Other major binders	CO_2 uptake at any time
Agarwal et al. 2023	100	0	0	NA	6.5 % (4 h)
	97	3	0	NA	9.7 % (4 h)
	95	5	0	NA	11 % (4 h)
	90	10	0	NA	4.8 % (4 h)

NA: Not available.

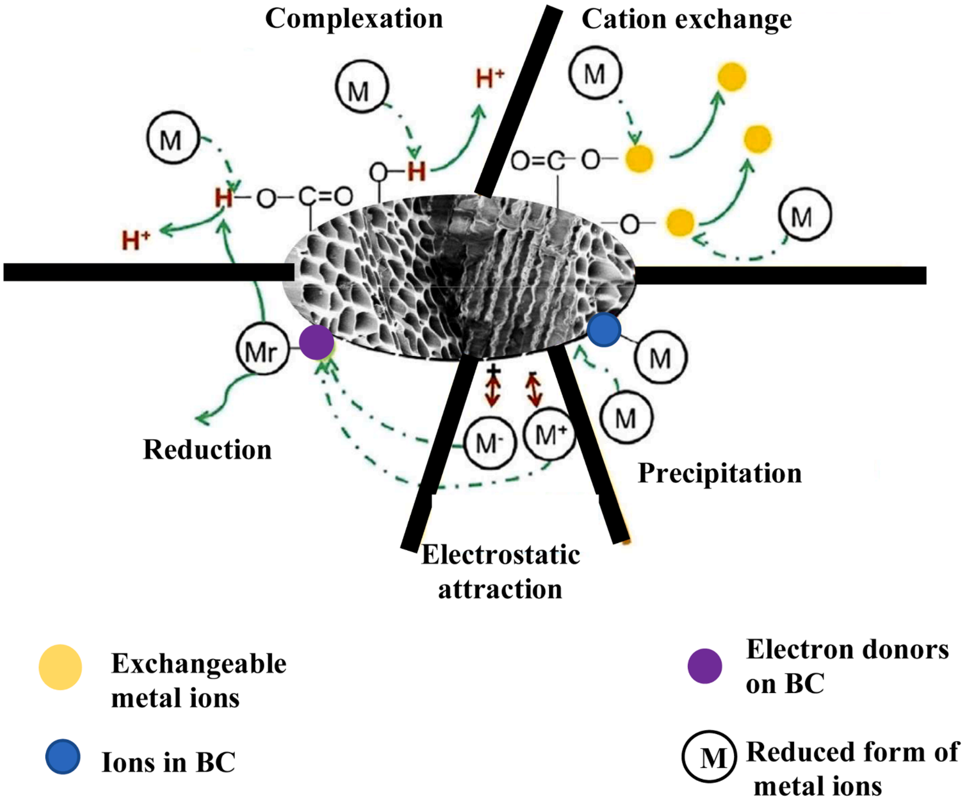

Fig. A1. Schematics showing CO_2 capture mechanisms of BC via different mechanisms (after Shafawi et al., 2021).

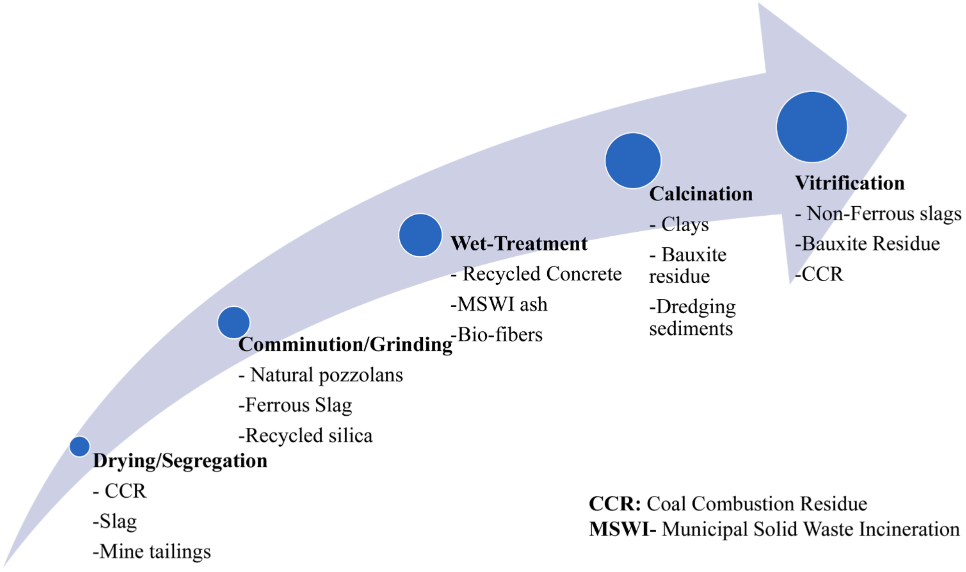

Fig. A2. Treatments for secondary cementitious materials for enhancing hydrate dissociation for carbonate precipitation.

Data availability

Data will be made available on request.

References

Abdullah M. Zeyad 2023. Sustainable concrete Production: incorporating recycled wastewater as a green building material, Volume 407, 1 December 2023, 133522, https://doi.org/10.1016/j.conbuildmat.2023.133522.

Agarwal, R., Pawar, N., Supriya, Rawat P., Rai, D., Kumar, R., Srinivasarao, N.B., 2023. Thermo-mechanical behavior of cementitious material with partial replacement of Class-II biochar with accelerated carbonation curing (ACC). Ind. Crops Prod. 204, 117335. https://doi.org/10.1016/j.indcrop.2023.117335. Part BISSN 0926-6690.

Akinyemi, B.A., Adesina, A., 2020. Recent advancements in the use of biochar for cementitious applications: a review. J. Build. Eng., 101705

Alaya, M.N., Girgis, B.S., Mourad, W.E., 2000. Activated carbon from some agricultural wastes under action of one-step steam pyrolysis. J. Porous Mater. 7 (4), 509–517. https://doi.org/10.1023/A:1009630928646.

Ali, Maisarah, Sufian Abdullah, Muhd, Saad, Siti Asmahani, 2015. Effect of calcium carbonate replacement on workability and mechanical strength of portland cement concrete. Adv. Mat. Res. 1115, 137–141. https://doi.org/10.4028/www.scientific.net/AMR.1115.137.

Angst, Ueli M., 2023. Steel corrosion in concrete – achilles' heel for sustainable concrete? Cement Concr. Res. 172, 107239. https://doi.org/10.1016/j.cemconres.2023.107239.

Antal, Michael Jerry, Grønli, Morten, 2003. The art, science, and technology of charcoal production. Ind. Eng. Chem. Res. 42 (8), 1619–1640. https://doi.org/10.1021/ie0207919.

Ashraf, Warda, Olek, Jan, 2016. Carbonation behavior of hydraulic and non-hydraulic calcium silicates: potential of utilizing low-lime calcium silicates in cement-based materials. J. Mater. Sci. 51 (13), 6173–6191. https://doi.org/10.1007/s10853-016-9909-4.

Baradaran S., Aliha M.R.M., Maleki A., Underwood B.S., 2024. Fracture properties of asphalt mixtures containing high content of reclaimed asphalt pavement (RAP) and eco-friendly PET additive at low temperature, Volume 449, 25 October 2024, 138426, https://doi.org/10.1016/j.conbuildmat.2024.138426.

Baradaran, S., Rahimi, J., Ameri, M., Maleki, A., 2024b. Mechanical performance of asphalt mixture containing eco-friendly additive by recycling PET. Case Stud. Construc. Mater. 20, e02740. https://doi.org/10.1016/j.cscm.2023.e02740. ISSN 2214-5095.

Boateng, A.A., 2007. Characterization and thermal conversion of charcoal derived from fluidized-bed fast pyrolysis oil production of switchgrass. Ind. Eng. Chem. Res. 46 (26), 8857–8862. https://doi.org/10.1021/ie071054l.

Brewer, Catherine E., Chuang, Victoria J., Masiello, Caroline A., Gonnermann, Helge, Gao, Xiaodong, Dugan, Brandon, Driver, Laura E., Panzacchi, Pietro, Zygourakis, Kyriacos, Davies, Christian A., 2014. New approaches to measuring biochar density and porosity. Biomass Bioener. 66, 176–185. https://doi.org/10.1016/j.biombioe.2014.03.059.

Brownsort, Peter A. 2009. "Biomass pyrolysis processes: performance parameters and their influence on biochar system benefits.".

Bruun, Esben W., Ambus, Per, Egsgaard, Helge, Hauggaard-Nielsen, Henrik, 2012. Effects of slow and fast pyrolysis biochar on soil C and N turnover dynamics. Soil Biol. Biochem. 46, 73–79. https://doi.org/10.1016/j.soilbio.2011.11.019.

Bullerjahn, F., Zajac, M., Pekarkova, J., Nied, D., 2020. Novel SCM produced by the co-calcination of aluminosilicates with dolomite. Cement Concr. Res. 134, 106083. https://doi.org/10.1016/j.cemconres.2020.106083. ISSN 0008-8846.

Cao, Mingli, Ming, Xing, He, Kaiyu, Li, Li, Shen, Shirley, 2019. Effect of macro-, micro- and nano-calcium carbonate on properties of cementitious composites—a review. Materials (Basel) 12 (5), 781. https://doi.org/10.3390/ma12050781.

Chen, L., Zhang, Y., Wang, L., Ruan, S., Chen, J., Li, H., Yang, J., Mechtcherine, V., Tsang, D.C.W., 2022a. Biochar-augmented carbon-negative concrete. Chem. Eng. J. 431, 133946. https://doi.org/10.1016/j.cej.2021.133946. Part 1ISSN 1385-8947.

Chen, T., Zhao, L., Gao, X., Li, L., Qin, L., 2022b. Modification of carbonation-cured cement mortar using biochar and its environmental evaluation. Cement Concr. Comp. 134, 104764. https://doi.org/10.1016/j.cemconcomp.2022.104764. ISSN 0958-9465.

Choi, Won Chang, Yun, Hyun Do, Lee, Jae Yeon, 2012. Mechanical properties of mortar containing bio-char from pyrolysis. J. Korea Inst. Struc. Mainten. Inspec. 16 (3), 67–74. https://doi.org/10.11112/jksmi.2012.16.3.067.

Clifford, A.A., Williams, J.R., 2000. Introduction to supercritical fluids and their applications. Method. Biotechnol.™ 13. https://doi.org/10.1385/1-59259-030-6:1. Humana Press.

Cross, A., Sohi, S.P., 2013. A method for screening the relative long-term stability of biochar. GCB Bioener. 5 (2), 215–220. https://doi.org/10.1111/gcbb.12035.

Cui, Hongzhi, Tang, Waiching, Liu, Wei, Dong, Zhijun, Xing, Feng, 2015. Experimental study on effects of CO2 concentrations on concrete carbonation and diffusion mechanisms. Construc. Build. Mater. 93, 522–527. https://doi.org/10.1016/j.conbuildmat.2015.06.007.

Das, S.K., Ghosh, G.K., Avasthe, R.K., Sinha, K., 2021. Compositional heterogeneity of different biochar: effect of pyrolysis temperature and feedstocks. J. Environ. Manage. 278. https://doi.org/10.1016/j.jenvman.2020.111501. Part 2, 111501ISSN 0301-4797.

Dilek, Angın, 2013. Effect of pyrolysis temperature and heating rate on biochar obtained from pyrolysis of safflower seed press cake. Bioresour. Technol. 128, 593–597. https://doi.org/10.1016/j.biortech.2012.10.150.

Dixit, A., Du, H., Pang, S.D., 2021. Carbon capture in ultra-high performance concrete using pressurized CO2 curing. Construc. Build. Mater. 288, 123076. https://doi.org/10.1016/j.conbuildmat.2021.123076. ISSN 0950-0618.

EN 1996-1-1: eurocode 6: design of mansonary structures. https://www.phd.eng.br/wp-content/uploads/2015/02/en.1996.1.1.2005.pdf.

Escobar, M.M., Di Paolo, A., Vazquez, A., 2013. Carbon dioxide uptake by concrete modified with carbon nanotube. In: Proceedings of the ASME 2013 32nd International Conference on Ocean, Offshore and Arctic Engineering. Volume 6: Polar and Arctic Sciences and Technology; Offshore Geotechnics; Petroleum Technology Symposium. ASME, V006T11A024. https://doi.org/10.1115/OMAE2013-11475. Nantes, France. June 9–14.

García-González, Carlos A., Hidalgo, A., Andrade, C., Alonso, M.C., Fraile, J., López-Periago, A.M., Domingo, C., 2006. Modification of composition and microstructure of portland cement pastes as a result of natural and supercritical carbonation procedures. Ind. Eng. Chem. Res. 45 (14), 4985–4992. https://doi.org/10.1021/ie0603363.

Gupta, S., Kua, H.W., 2018. Effect of water entrainment by pre-soaked biochar particles on strength and permeability of cement mortar. Constr. Build. Mater. 159, 107–125.

Gupta, Souradeep, Kua, Harn Wei, Cynthia, Sin Yee Tan, 2017a. Use of biochar-coated polypropylene fibers for carbon sequestration and physical improvement of mortar. Cement Concrete Compos. 83, 171–187. https://doi.org/10.1016/j.cemconcomp.2017.07.012.

Factors determining the potential of biochar as a carbon capturing and sequestering construction material. Critical Rev. J. Mater. Civil Eng. 29 (9), 2017. Retrieved January 16, 2024.

Gupta, Souradeep, Kashani, Alireza, Hasan Mahmood, Aziz, Han, Tianhao, 2021. Carbon sequestration in cementitious composites using biochar and fly ash – effect on mechanical and durability properties. Construc. Build. Mater. 291, 123363. https://doi.org/10.1016/j.conbuildmat.2021.123363.

Han, L., Zhang, B., Chen, L., Feng, Y., Yang, Y., Sun, K., 2021. Impact of biochar amendment on soil aggregation varied with incubation duration and biochar pyrolysis temperature. Biochar 3 (3), 339–347.

Hanafi, M., Bordoloi, S., Rinta-Hiiro, V., Oey, T., Korkiala-Tanttu, L., 2024. Feasibility of biochar for low-emission soft clay stabilization using CO2 curing. Transp. Geotech. 49, 101370.

Hu, Xin, Radosz, Maciej, Cychosz, Katie A., Thommes, Matthias, 2011. CO2-filling capacity and selectivity of carbon nanopores: synthesis, texture, and pore-size distribution from quenched-solid density functional theory (QSDFT). Environ. Sci. Technol. 45 (16), 7068–7074. https://doi.org/10.1021/es200782s.

Jang, H.W., Yang, D., 2023. Determination of the concentration-dependent effective diffusivity of CO2 in unconsolidated porous media saturated with heavy oil by considering the swelling effect. Int. J. Heat Mass Transf. 201, 123552. Part 2.

Jansen, R.J.J., van Bekkum, H., 1994. Amination and ammoxidation of activated carbons. Carbon N Y 32 (8), 1507–1516. https://doi.org/10.1016/0008-6223(94)90146-5.

Jhatial, A.A., Nováková, I., Gjerløw, E.A., 2023. Review on emerging cementitious materials, reactivity evaluation and treatment methods. Buildings 13, 526. https://doi.org/10.3390/buildings13020526.

Jia, B., Tsau, J.S., Barati, R., 2019. Measurement of CO2 diffusion coefficient in the oil-saturated porous media. J. Petrol. Sci. Eng. 181, 106189. https://doi.org/10.1016/j.petrol.2019.106189. ISSN 0920-4105.

John and Lothenbach 2023, "Cement hydration mechanisms through time – a review | Journal of Materials Science." Retrieved December 25, 2023 (https://link.springer.com/article/10.1007/s10853-023-08651-9).

Khan M. and McNally C. 2023. A holistic review on the contribution of civil engineers for driving sustainable concrete construction in the built environment, Volume 16, December 2023, 100273, https://doi.org/10.1016/j.dibe.2023.100273.

Kheirinik, M., Ahmed, S., Rahmanian, N., 2021. Comparative techno-economic analysis of carbon capture processes: pre-combustion, post-combustion, and oxy-fuel combustion operations. Sustainability 13, 13567. https://doi.org/10.3390/su132413567.

Kim, Min-Koo, Wang, Qian, Li, Heng, 2019. Non-contact sensing based geometric quality assessment of buildings and civil structures: a review. Autom. Construc. 100, 163–179. https://doi.org/10.1016/j.autcon.2019.01.002.

Kua, H.W., Tan, S.M.H., 2023. Novel typology of accelerated carbonation curing: using dry and pre-soaked biochar to tune carbon capture and mechanical properties of cementitious mortar. Biochar 5, 36. https://doi.org/10.1007/s42773-023-00234-w.

Langley L.A., and Fairbrother D.H., 2007. Effect of wet chemical treatments on the distribution of surface oxides on carbonaceous materials. doi:10.1016/j.carbon.2006.08.008.

Lemonis, N., Tsakiridis, P.E., Katsiotis, N.S., Antiohos, S., Papageorgiou, D., Katsiotis, M.S., Beazi-Katsioti, M., 2015. Hydration study of ternary blended cements containing ferronickel slag and natural pozzolan. Construc. Build. Mater. 81, 130–139. https://doi.org/10.1016/j.conbuildmat.2015.02.046. ISSN 0950-0618.

Li, L., Wu, M., 2022. An overview of utilizing CO2 for accelerated carbonation treatment in the concrete industry. J. CO2 Utiliz. 60, 102000. June 2022.

Li, S., Li, Z., Dong, Q., 2016. Diffusion coefficients of supercritical CO2 in oil-saturated cores under low permeability reservoir conditions. J. CO2 Utiliz. 14, 47–60. https://doi.org/10.1016/j.jcou.2016.02.002. ISSN 2212-9820.

Li, Jing, Yu, Qijun, Huang, Haoliang, Yin, Suhong, 2019. Effects of Ca/Si Ratio, aluminum and magnesium on the carbonation behavior of calcium silicate hydrate. Materials (Basel, Switzerland) 12 (8), 1268. https://doi.org/10.3390/ma12081268.

Liu, J., Zeng, C., Li, Z., Liu, G., Zhang, W., Xie, G., Xing, F., 2023. Carbonation of steel slag at low CO2 concentrations: novel biochar cold-bonded steel slag artificial aggregates. Sci. Total Environ. 902, 166065. https://doi.org/10.1016/j.scitotenv.2023.166065. ISSN 0048-9697.

Madzaki, H., KarimGhani, W.A.W.A., 2016. Carbon dioxide adsorption on sawdust biochar. Procedia Eng. 148, 718–725.

Mishra, Geetika, Danoglidis, Panagiotis, Shah, Surendra P., Konsta-Gdoutos, Maria, 2023a. Carbon capture and storage potential of biochar-enriched cementitious systems. Cement Concrete Compos. 140, 105078.

Mishra, Geetika, Danoglidis, Panagiotis, Shah, Surendra P., Konsta-Gdoutos, Maria, 2023b. Optimization of biochar and fly ash to improve mechanical properties and CO2 sequestration in cement mortar. Construc. Build. Mater. 392, 132021. https://doi.org/10.1016/j.conbuildmat.2023.132021.

Munroe, Adriana, Downie, Alan, Crosky, Paul., 2009. Physical Properties of Biochar. Biochar for Environmental Management. Routledge.

Nan, H., Zhao, L., Yang, F., Liu, Y., Xiao, Z., Cao, X., Qiu, H., 2020. Different alkaline minerals interacted with biomass carbon during pyrolysis: which one improved biochar carbon sequestration? J. Clean Prod 255, 120162.

Newalkar, Gautami, Iisa, Kristiina, D'Amico, Andrew D., Sievers, Carsten, Agrawal, Pradeep, 2014. Effect of temperature, pressure, and residence time on pyrolysis of pine in an entrained flow reactor. Ener. Fuels 28 (8), 5144–5157. https://doi.org/10.1021/ef5009715.

Ngo, D.N.G., Chuang, X.Y., Huang, C.P., Hua, L.C., Huang, C., 2023. Compositional characterization of nine agricultural waste biochars: the relations between alkaline metals and cation exchange capacity with ammonium adsorption capability. J. Environ. Chem. Eng. 11 (3), 110003. https://doi.org/10.1016/j.jece.2023.110003. ISSN 2213-3437.

Nikolai, P., Rabiyat, B., Aslan, A., et al., 2019. Supercritical CO_2: properties and technological applications - a review. J. Therm. Sci. 28, 394–430. https://doi.org/10.1007/s11630-019-1118-4.

Nilimaa, J., 2023. Smart materials and technologies for sustainable concrete construction. Develop. Built Environ. 15, 100177. https://doi.org/10.1016/j.dibe.2023.100177. ISSN 2666-1659.

Okumura, Yukihiko, Hanaoka, Toshiaki, Sakanishi, Kinya, 2009. Effect of pyrolysis conditions on gasification reactivity of woody biomass-derived char. Proc. Combust. Inst. 32 (2), 2013–2020. https://doi.org/10.1016/j.proci.2008.06.024.

Pan, S.Y., Chiang, P.C., Pan, W., Kim, H., 2018. Advances in state-of-art valorization technologies for captured CO_2 toward sustainable carbon cycle. Crit. Rev. Environ. Sci. Technol. 48 (5), 471–534. https://doi.org/10.1080/10643389.2018.1469943.

Papadakis, Vagelis G, 2000. Effect of supplementary cementing materials on concrete resistance against carbonation and chloride ingress. Cement Concr. Res. 30 (2), 291–299. https://doi.org/10.1016/S0008-8846(99)00249-5.

Pariyar, P., Kumari, K., Jain, M.K., Jadhao, P.S., 2020. Evaluation of change in biochar properties derived from different feedstock and pyrolysis temperature for environmental and agricultural application. Sci. Total Environ. 713, 136433. https://doi.org/10.1016/j.scitotenv.2019.136433. ISSN 0048-9697.

Pimentel, C.H., Díaz-Fernández, L., Gómez-Díaz, D., Freire, M.S., González-Álvarez, J., 2023. Separation of CO2 using biochar and KOH and ZnCl2 activated carbons derived from pine sawdust. J. Environ. Chem. Eng. 11 (6), 111378.

Plaza, M.G., González, A.S., Pis, J.J., Rubiera, F., Pevida, C., 2014. Production of microporous biochars by single-step oxidation: effect of activation conditions on CO2 capture. Appl. Energy 114, 551–562. https://doi.org/10.1016/j.apenergy.2013.09.058.

Poucke, R.V., Allaert, S., Ok, Y.S., Pala, M., Ronsse, F., Tack, F.M.G., Meers, E., 2019. Metal sorption by biochars: a trade-off between phosphate and carbonate concentration as governed by pyrolysis conditions. J. Environ. Manage. 246, 496–504. https://doi.org/10.1016/j.jenvman.2019.05.112. ISSN 0301-4797.

Power, Ian M. and Paulo, Carlos and Long, Hannah and Lockhart, Justin A. and Stubbs, Amanda R. and French, David and Caldwell, Robert, 2021. Carbonation, cementation, and stabilization of ultramafic mine tailings. doi: 10.1021/acs.est.1c01570.

Praneeth, Sai, Guo, Ruonan, Wang, Tao, Dubey, Brajesh K., Sarmah, Ajit K., 2020. Accelerated carbonation of biochar reinforced cement-fly ash composites: enhancing and sequestering CO2 in building materials. Construc. Build. Mater. 244, 118363. https://doi.org/10.1016/j.conbuildmat.2020.118363.

Presser, Volker, McDonough, John, Yeon, Sun-Hwa, Gogotsi, Yury, 2011. Effect of pore size on carbon dioxide sorption by carbide derived carbon. Energy Environ. Sci. 4 (8), 3059–3066. https://doi.org/10.1039/C1EE01176F.

Reyes G., Vega-Coloma M., Antonova A., Ajdary R., Jonveaux S., Flanigan C., Lautenbacher N., and Rojas O.J., 2023. Direct CO2 capture by alkali-dissolved cellulose and sequestration in building materials and artificial reef structures. https://doi.org/10.1002/adma.202209327.

Rezk, M.G., Foroozesh, J., 2019. Effect of CO2 mass transfer on rate of oil properties changes: application to CO2-EOR projects. J. Petrol. Sci. Eng 180, 298–309. September 2019.

Roberts, Kelli G., Gloy, Brent A., Joseph, Stephen, Scott, Norman R., Lehmann, Johannes, 2010. Life cycle assessment of biochar systems: estimating the energetic, economic, and climate change potential. Environ. Sci. Technol. 44 (2), 827–833. https://doi.org/10.1021/es902266r.

Rodriguez-Reinoso, F., Molina-Sabio, M., González, M.T., 1995. The use of steam and CO2 as activating agents in the preparation of activated carbons. Carbon 33 (1), 15–23.

Rodríguez-Reinoso, F., Molina-Sabio, M., 1992. Activated carbons from lignocellulosic materials by chemical and/or physical activation: an overview. Carbon N Y 30 (7), 1111–1118. https://doi.org/10.1016/0008-6223(92)90143-K.

Sathiparan N., Anburuvel A., Selvam V.V., 2023. Utilization of agro-waste groundnut shell and its derivatives in sustainable construction and building materials – a review, Volume 66, 1 May 2023, 105866, https://doi.org/10.1016/j.jobe.2023.105866.

Schröder, Elisabeth, Thomauske, Klaus, Weber, Christine, Hornung, Andreas, Tumiatti, Vander, 2007. Experiments on the generation of activated carbon from biomass. J. Anal. Appl. Pyrolys. 79 (1), 106–111. https://doi.org/10.1016/j.jaap.2006.10.015.

Sevilla, Marta, Fuertes, Antonio B., 2011. Sustainable porous carbons with a superior performance for CO2 capture. Energy Environ. Sci. 4, 1765. https://doi.org/10.1039/C0EE00784F.

Shaaban, A., Se, Sian-Meng, Mitan, Nona Merry M., Dimin, M.F., 2013. Characterization of biochar derived from rubber wood sawdust through slow pyrolysis on surface porosities and functional groups. Procedia Eng. 68, 365–371. https://doi.org/10.1016/j.proeng.2013.12.193.

Shafeeyan, Mohammad Saleh, Daud, Wan Mohd Ashri Wan, Houshmand, Amirhossein, Arami-Niya, Arash, 2011. Ammonia modification of activated carbon to enhance carbon dioxide adsorption: effect of pre-oxidation. Appl. Surf. Sci. 257 (9), 3936–3942. https://doi.org/10.1016/j.apsusc.2010.11.127.

Sharma, D., Goyal, S., 2018. Accelerated carbonation curing of cement mortars containing cement kiln dust: an effective way of CO2 sequestration and carbon footprint reduction. J. Clean Prod 192, 844e854, 2018.

Sharma, A., Jindal, J., Mittal, A., et al., 2021. Carbon materials as CO_2 adsorbents: a review. Environ. Chem. Lett. 19, 875–910. https://doi.org/10.1007/s10311-020-01153-z.

Sikora, Pawel, Woliński, Paweł, Chougan, Mehdi, Madraszewski, Szymon, Węgrzyński, Wojciech, Papis, Bartłomiej K., Federowicz, Karol, Ghaffar, Seyed Hamidreza, Stephan, Dietmar, 2022. A Systematic experimental study on biochar-cementitious composites: towards carbon sequestration. Ind. Crops Prod. 184, 115103. https://doi.org/10.1016/j.indcrop.2022.115103.

Sohi, S.P., Krull, E., Lopez-Capel, E., Bol, R., 2010. Chapter 2 - a review of biochar and its use and function in soil. Advances in Agronomy. Academic Press, pp. 47–82. Vol. 105Advances in Agronomy.

Song, S., Liu, Z., Liu, G., Cui, X., Sun, J., 2023. Application of biochar cement-based materials for carbon sequestration. Construc. Build. Mater. 405, 133373.

Sun, Yining, Gao, Bin, Yao, Ying, Fang, June, Zhang, Ming, Zhou, Yanmei, Chen, Hao, Yang, Liuyan, 2014. Effects of feedstock type, production method, and pyrolysis temperature on biochar and hydrochar properties. Chem. Eng. J. 240, 574–578. https://doi.org/10.1016/j.cej.2013.10.081.

Tajra, F., Elrahman, M.A., Stephan, D., 2019. The production and properties of cold-bonded aggregate and its applications in concrete: a review. Construc. Build. Mater. 225, 29–43. https://doi.org/10.1016/j.conbuildmat.2019.07.219. ISSN 0950-0618.

Tomczyk, A., Sokołowska, Z., Boguta, P., 2020. Biochar physicochemical properties: pyrolysis temperature and feedstock kind effects. Rev. Environ. Sci. Biotechnol. 19, 191–215. https://doi.org/10.1007/s11157-020-09523-3.

Wang, Y., Liu, Y., Zhan, W., Zheng, K., Wang, J., Zhang, C., Chen, R., 2020. Stabilization of heavy metal-contaminated soils by biochar: challenges and recommendations. Sci. Total Environ. 729, 139060. https://doi.org/10.1016/j.scitotenv.2020.139060. ISSN 0048-9697.

Wang, L., Chen, L., Poon, C.S., Wang, C.H., Ok, Y.S., Mechtcherine, V., Tsang, D.C.W., 2021. Roles of biochar and CO2 curing in sustainable magnesia cementbased composites. ACS Sustain. Chem. Eng. 9, 8603–8610.

Wei, Haoran, Deng, Shubo, Hu, Bingyin, Chen, Zhenhe, Wang, Bin, Huang, Jun, Yu, Gang, 2012. Granular bamboo-derived activated carbon for high CO2 adsorption: the dominant role of narrow micropores. ChemSusChem 5 (12), 2354–2360. https://doi.org/10.1002/cssc.201200570.

Williams, Paul T., Reed, Anton R., 2004. High grade activated carbon matting derived from the chemical activation and pyrolysis of natural fibre textile waste. J. Anal. Appl. Pyrolysis 71 (2), 971–986. https://doi.org/10.1016/j.jaap.2003.12.007.

J Xie, X., Economides, M.J., 2009. The impact of carbon geological sequestration. J. Nat. Gas Sci. Eng. 1, 103–111, 2009.

Xiong, Zhang, Shihong, Zhang, Haiping, Yang, Tao, Shi, Yingquan, Chen, Hanping, Chen, 2013. Influence of NH3/CO2 modification on the characteristic of biochar and the CO2 capture. Bioener. Res. 6 (4), 1147–1153. https://doi.org/10.1007/s12155-013-9304-9.

Xu, Maochun, Zhang, Yuyang, Yang, Shuo, Mo, Liwu, Liu, Peng, 2023. Effects of internal CO2 curing provided by biochar on the carbonation and properties of steel slag-based artificial lightweight aggregates (SALAs). Cement Concr. Comp. 142, 105197. https://doi.org/10.1016/j.cemconcomp.2023.105197.

Yang, Xu, Wang, Xiao-Yong, 2021. Strength and durability improvements of biochar-blended mortar or paste using accelerated carbonation curing. J. CO2 Utiliz. 54, 101766. https://doi.org/10.1016/j.jcou.2021.101766.

Yoon, In-Seok, Chang, Chun-Ho, 2020. Time evolution of CO2 diffusivity of carbonated concrete. Appl. Sci. 10 (24), 8910. https://doi.org/10.3390/app10248910.

Yuan, Haoran, Lu, Tao, Wang, Yazhuo, Huang, Hongyu, Chen, Yong, 2014. Influence of pyrolysis temperature and holding time on properties of biochar derived from medicinal herb (radix isatidis) residue and its effect on soil CO2 emission. J. Anal. Appl. Pyrolysis 110, 277–284. https://doi.org/10.1016/j.jaap.2014.09.016.

Zajac, M., Skibsted, J., Durdzinski, P., Bullerjahn, F., Skocek, J., Haha, M.B., 2020. Kinetics of enforced carbonation of cement paste. Cement Concr. Res. 131, 106013. https://doi.org/10.1016/j.cemconres.2020.106013. ISSN 0008-8846.

Zhang, Jie, Liu, Jia, Liu, Rongle, 2015. Effects of pyrolysis temperature and heating time on biochar obtained from the pyrolysis of straw and lignosulfonate. Bioresour. Technol. 176, 288–291. https://doi.org/10.1016/j.biortech.2014.11.011.

Zhang, A., Li, X., Xing, J., Xu, G., 2020. Adsorption of potentially toxic elements in water by modified biochar: a review. J. Environ. Chem. Eng. 8 (4), 104196. https://doi.org/10.1016/j.jece.2020.104196. ISSN 2213-3437.

Zhang, Y., Wang, S., Feng, D., Gao, J., Dong, L., Zhao, Y., Sun, S., Huang, Y., Qin, Y., 2022. Functional biochar synergistic solid/liquid-phase CO2 capture: a review. : Energy Fuels 36, 2945–2970, 2022.

Zhang, S., Yuan, Q., Ni, J., Zheng, K., Xu, Y., Zhang, J., 2023. CO2 utilization and sequestration in ready-mix concrete—a review. Sci. Total Environ., 168025

Zhao, Z., El-Naggar, A., Kau, J., et al., 2024a. Biochar affects compressive strength of Portland cement composites: a meta-analysis. Biochar 6 (21). https://doi.org/10.1007/s42773-024-00309-2.

Zhao, L., Zaborowski, E., Bordoloi, S., Rajagopalan, N., Sharma, B.K., Baroi, C., Xing, W., Zhang, L., 2024b. Characterization of novel polysulfide polymer coated fly ash and its application in mitigating diffusion of contaminants. Environ. Pollution 347, 123706. https://doi.org/10.1016/j.envpol.2024.123706. ISSN 0269-7491.

Zuo, W., Zhao, X., Luo, J., He, Z., Zhao, J., 2024. Investigating the impact of carbonation curing concentrations on the mechanical properties and microstructure of recycled concrete. J. Build. Eng. 96, 110465. https://doi.org/10.1016/j.jobe.2024.110465. ISSN 2352-7102.